中国科学院高能物理研究所
Institute of High Energy Physics, Chinese Academy of Sciences
中国高等科学技术中心
China Center of Advanced Science and Technology

Measurement of $\Xi^-/\bar{\Xi}^+$ production in jets from Z boson decays with DELPHI Open Data

Yuzhi CHE (车逾之)
Institute of High Energy Physics, Chinese Academy of Sciences
China Center of Advanced Science and Technology

Zhouyue Fan, Xinchou Lou, Zhaoru Zhang, Jinfei Wu, Gengyuan Zhang, Gang Li, Yanping Huang, and Manqi Ruan

arXiv:2607.13804

中国物理学会高能物理分会第十二届全国会员代表大会暨学术年会, 2026

LEP and DELPHI Open Data

The Large Electron-Positron (LEP) collider is **the largest electron-positron accelerator** ever built.

- Two operations from 1990 to 2000: **LEP I** (1990~1995, $91.2\,\mathrm{GeV}$) and **LEP II** (1996~2000, 161~$205\,\mathrm{GeV}$).
- Four detectors on LEP: **DELPHI**, ALEPH, OPAL and L3.

In 2024, the DELPHI collaboration decided to open the data and original software stack to the physics community **for public access** (see *DELPHI data preservation, re-use, and open access policy*) :

- original DELPHI analysis framework
- simulation & reconstruction
- the event display
- and documentation.

Other experiments' datasets are archived on EOS awaiting similar release (see *4th DPHEP Collaboration Workshop*).

Table 2
Overview of LEP performance from 1989 to 2000. $\int \mathcal{L}dt$ is the luminosity integrated per experiment over each year and I_{tot} is the total beam current $2k_\mathrm{b}I_\mathrm{b}$. The luminosity $\mathcal{L}$ is given in units of $10^{30}\mathrm{cm}^{-2}\,\mathrm{s}^{-1}$.

Year	$\int \mathcal{L}dt$ (pb^{-1})	E_b ($\mathrm{GeV/c^2}$)	k_b	I_{tot} (mA)	$\mathcal{L}$
1989	1.74	45.6	4	2.6	4.3
1990	8.6	45.6	4	3.6	7
1991	18.9	45.6	4	3.7	10
1992	28.6	45.6	4/8	5.0	11.5
1993	40.0	45.6	8	5.5	19
1994	64.5	45.6	8	5.5	23.1
1995	46.1	45.6	8/12	8.4	34.1
1996	24.7	80.5 - 86	4	4.2	35.6
1997	73.4	90 - 92	4	5.2	47.0
1998	199.7	94.5	4	6.1	100
1999	253	98 - 101	4	6.2	100
2000	233.4	102 - 104	4	5.2	60

CERN-SL-2002-009-OP

Hadron Production in Jets

- Gluon jets are expected to exhibit stronger color radiation in the perturbative parton cascade and to contain larger particle multiplicities.

- The ratios of K_S^0 and Λ production rates in gluon and quark jets relative to the mean charged particle multiplicity,

$$\mathscr{R}^h_{g/q} \equiv \frac{\langle N_h \rangle_g}{\langle N_{\rm ch} \rangle_g} \Bigg/ \frac{\langle N_h \rangle_q}{\langle N_{\rm ch} \rangle_q}$$

Identified strange-particle productions in gluon jets cannot be fully understood through a general scaling.

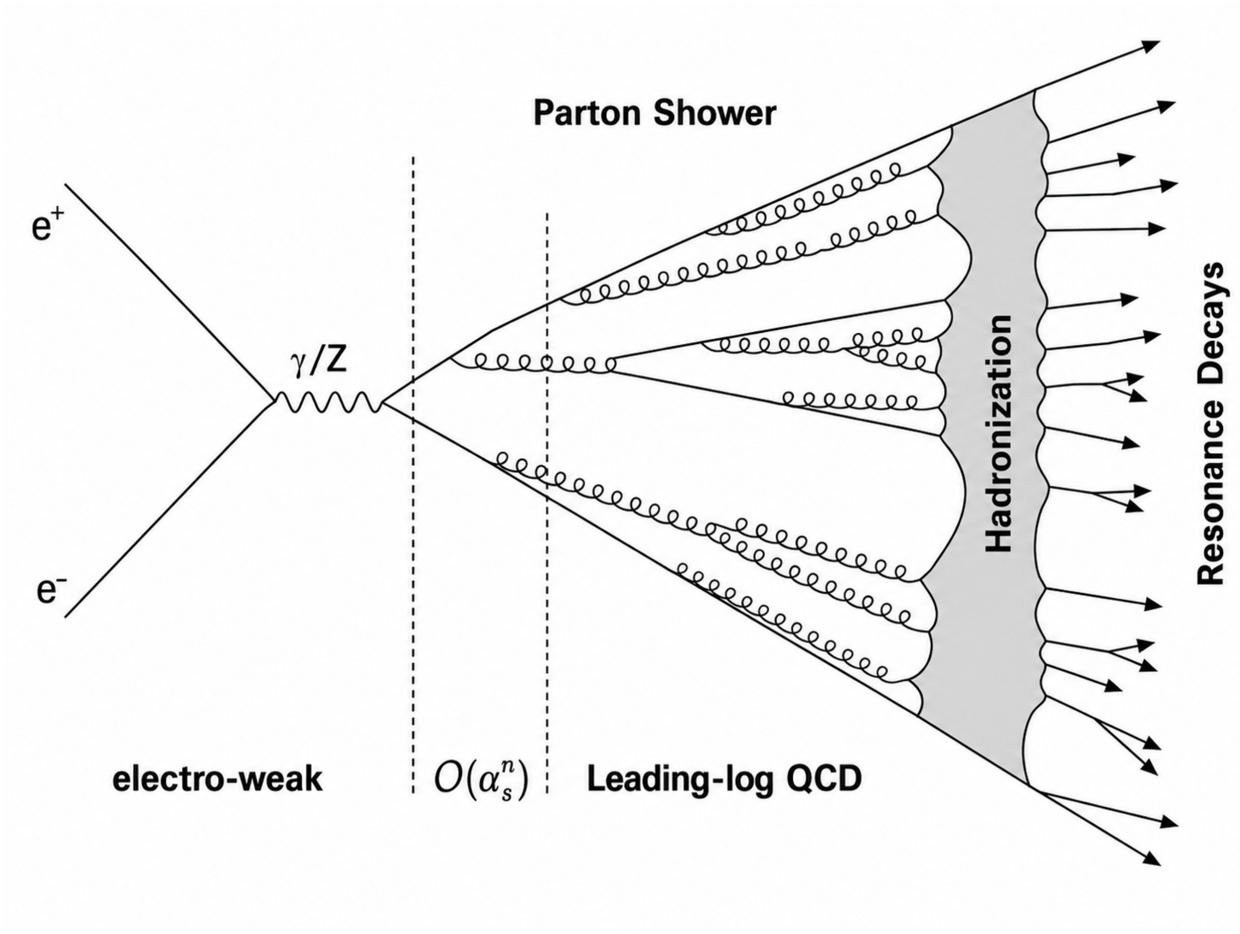

Z.Phys.C 70 (1996) 179–196

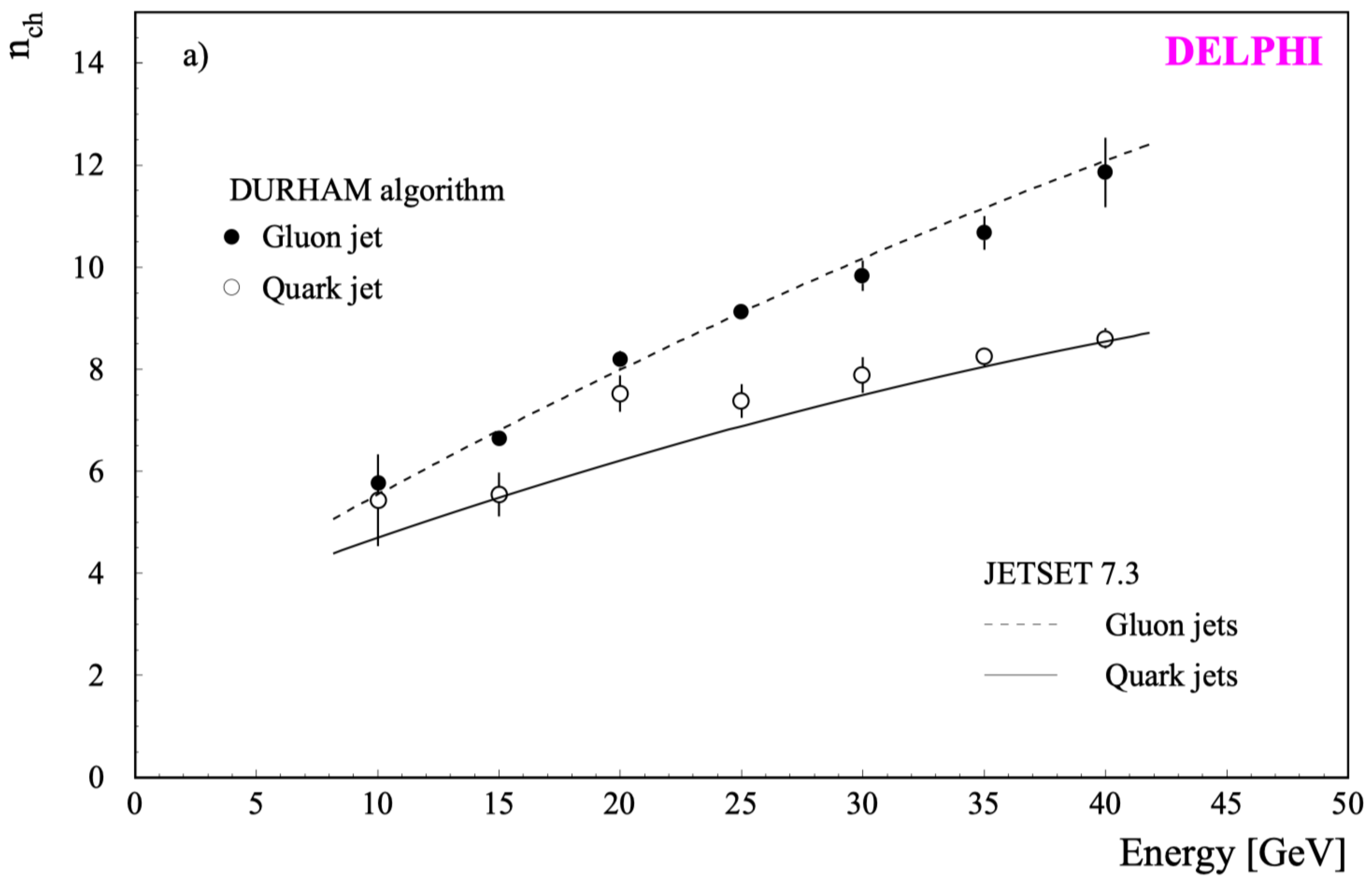

Eur.Phys.J.C 8 (1999) 241–254

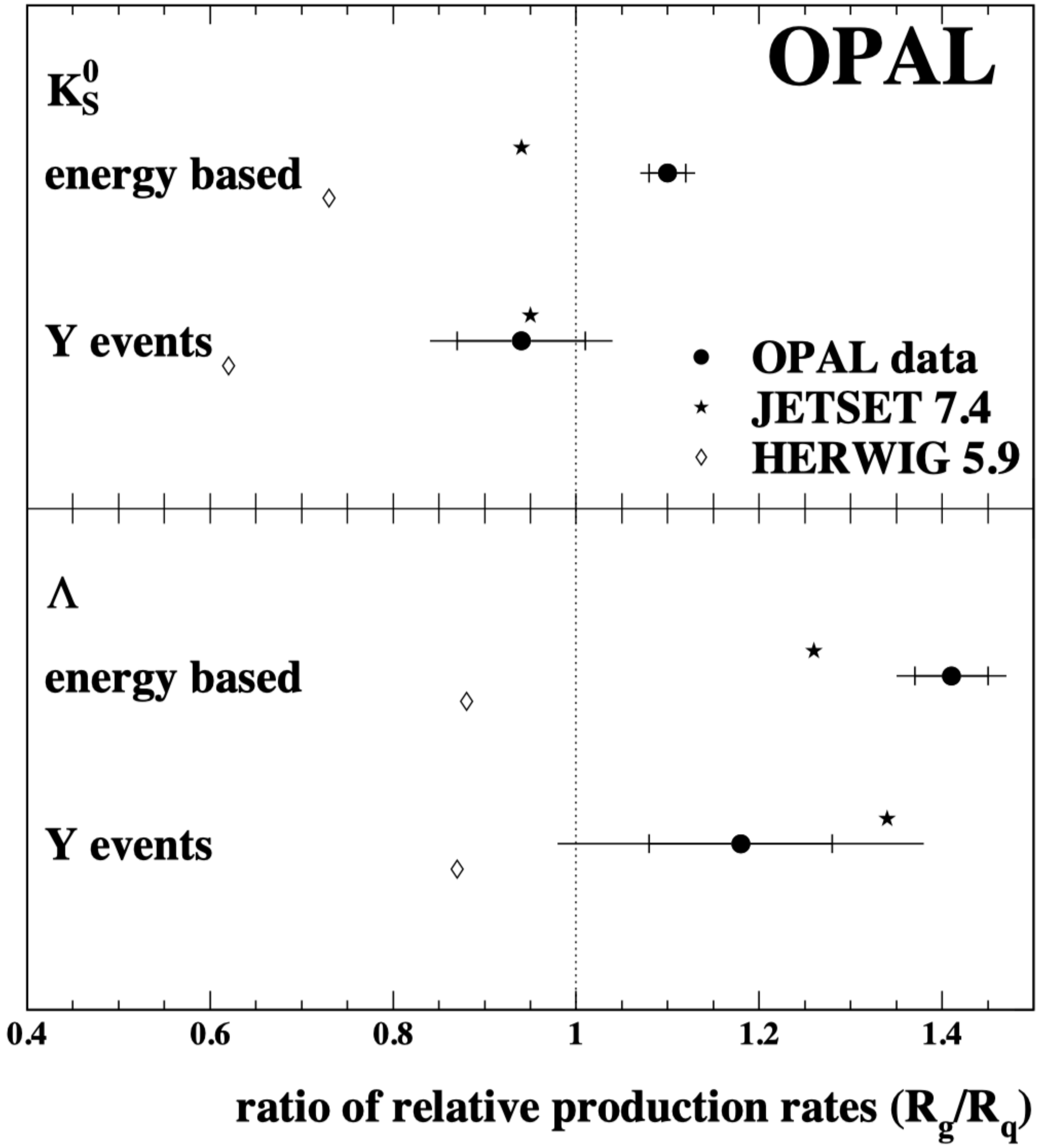

Fig. 7. The ratio of relative production rates (see text) in quark and gluon jets of K^0_S and Λ for both analyses. The experimental statistical errors are delimited by the small vertical bars. The predictions of JETSET 7.4 and HERWIG 5.9 are also shown. The predictions of JETSET 7.3 are no more than 0.04 lower than those of JETSET 7.4

Hadron Production in jets

The rapidity correlations between Λ baryons with other particles are observed.

There is local compensation mechanism during the production of strange quark and baryons.

The production of Ξ^- baryons in jets intrinsically involves the local compensation of strangeness and baryon number, making it a sensitive probe of non-perturbative QCD.

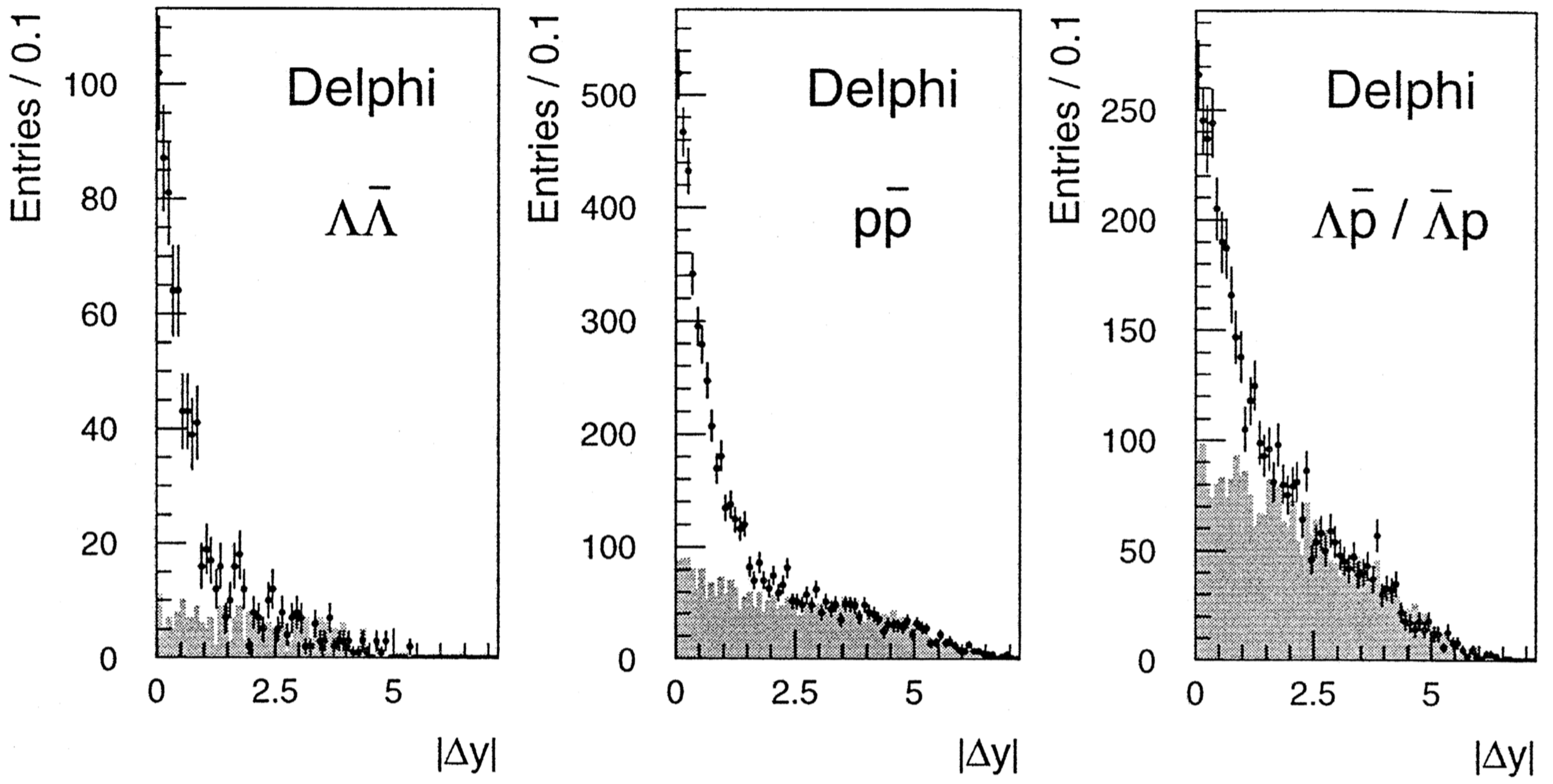

Fig. 2. Rapidity differences of baryon-antibaryon pairs (points with error bars) compared to those of baryon-baryon and antibaryon-anti-baryon pairs (shaded histograms) from Delphi data.

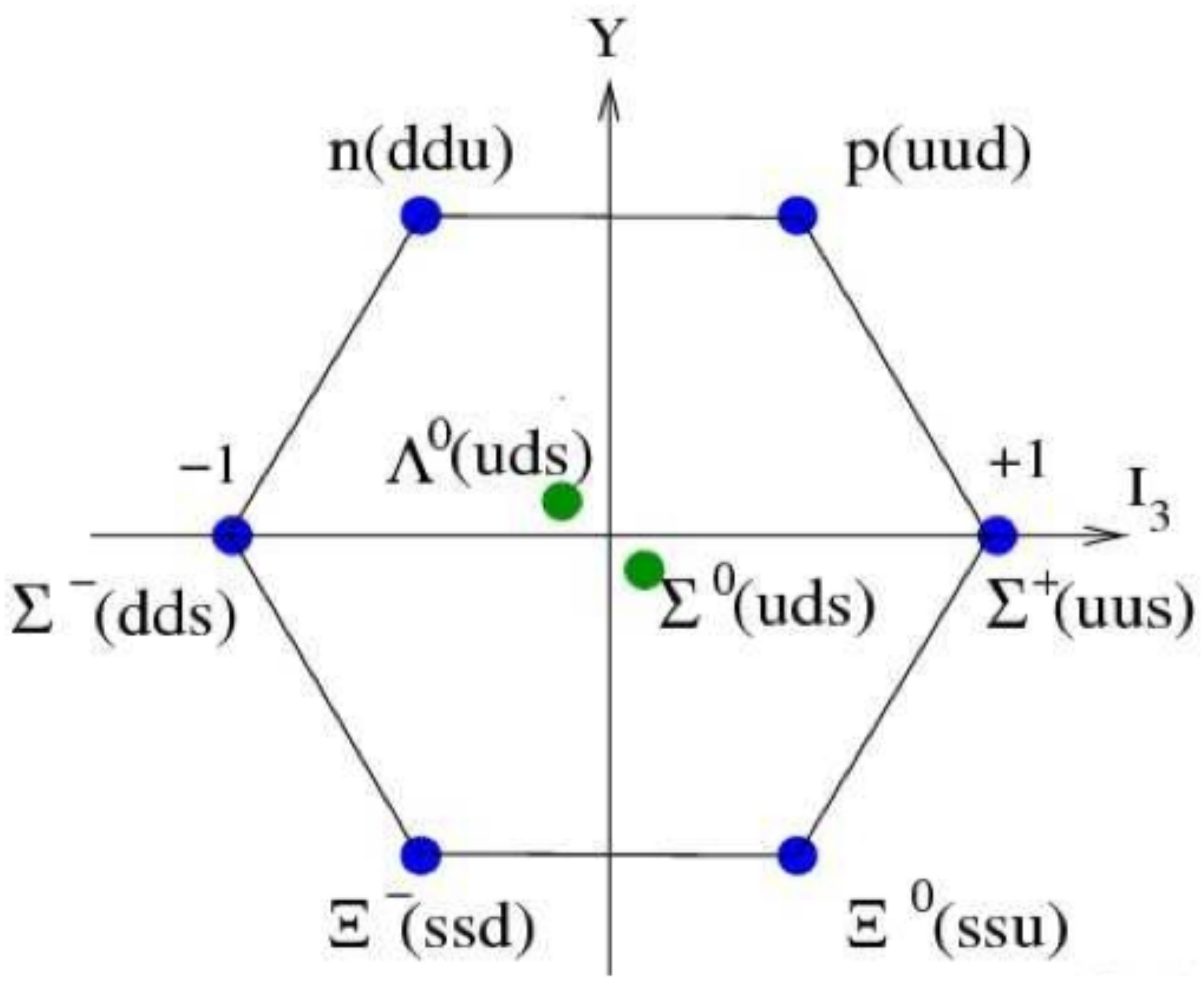

Data & MC Samples

- **Data:** Z decay samples collected during 1992-1995.
- **MC:** official inclusive $Z \rightarrow$ hadrons MC samples generated by JETSET

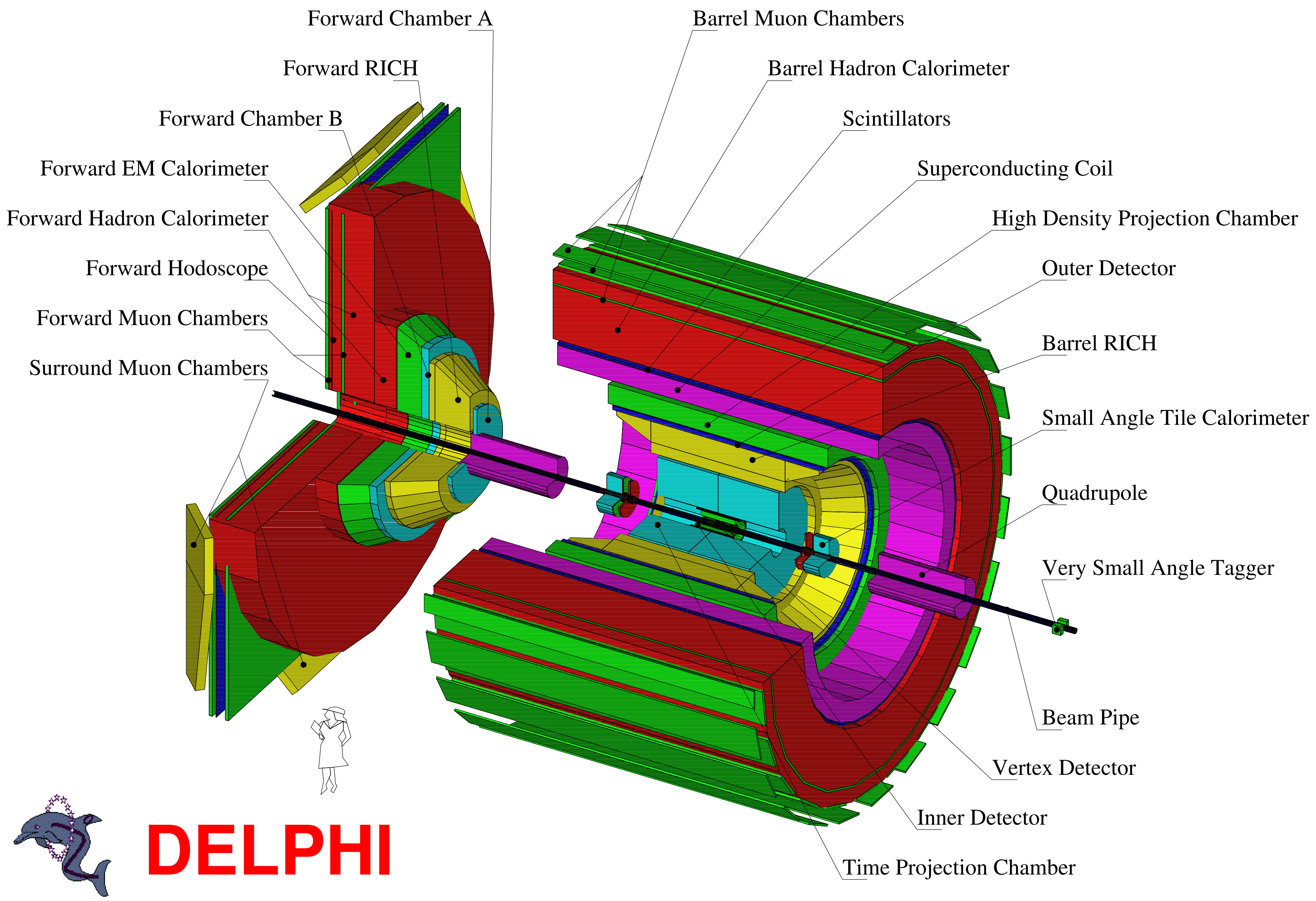

DELPHI

TABLE I. The nicknames and Digital Object Identifiers (DOI) of the used data sets and official simulation samples.

Type	Year	Sample	DOI
Data	1992	short92_e2	[17]
Data	1993	short93_d2	[18]
Data	1994	short94_c2	[19]
Data	1995	short95_d2	[20]
MC	1992	sh_kk2f4146qqpy_e91.25_c92_2l_e2	[21]
MC	1993	sh_kk2f4146qqpy_e91.25_c93_2l_d2	[22]
MC	1994	sh_kk2f4146qqpy_e91.25_l94_2l_c2	[23]
MC	1995	sh_kk2f4146qqpy_e91.25_c95_1l_d2	[24]

	Magnet Field	Tracking system	PID	ECAL	HCAL	Muon system
DELPHI	1.2 T (R ~ 2.6 m)	VTX, Inner drift, TPC, Outer drift, (~ 3%) (R: ~ 1.2 m)	dE/dx, dual-radiator RICH	HGC (~23%/$E^{0.5}$ ⊕ 1.1%)	Iron + streamer tubes	

Jet Clustering: Durham Algorithm

Repeat energy ranking method implemented in L3 (Phys.Lett.B 407 (1997) 389-401)/OPAL (Eur.Phys.J.C 8 (1999) 241-254).

Three/Two-jet events have been selected by official cuts for **track quality** and for the **hadronic event type** as well as applying a $k_\perp$ cluster algorithm (Durham).

Durham ($k_\perp$) algorithm via FastJet: iterative pairwise clustering of all accepted charged and neutral objects.

Distance: $y_{ij} = \dfrac{2\,\min(E_i^2, E_j^2)\,(1-\cos\theta_{ij})}{Q^2}$, where $Q = \sqrt{s} = 91.2\,\mathrm{GeV}$; Jet resolution parameter: $y_{cut} = 0.005$

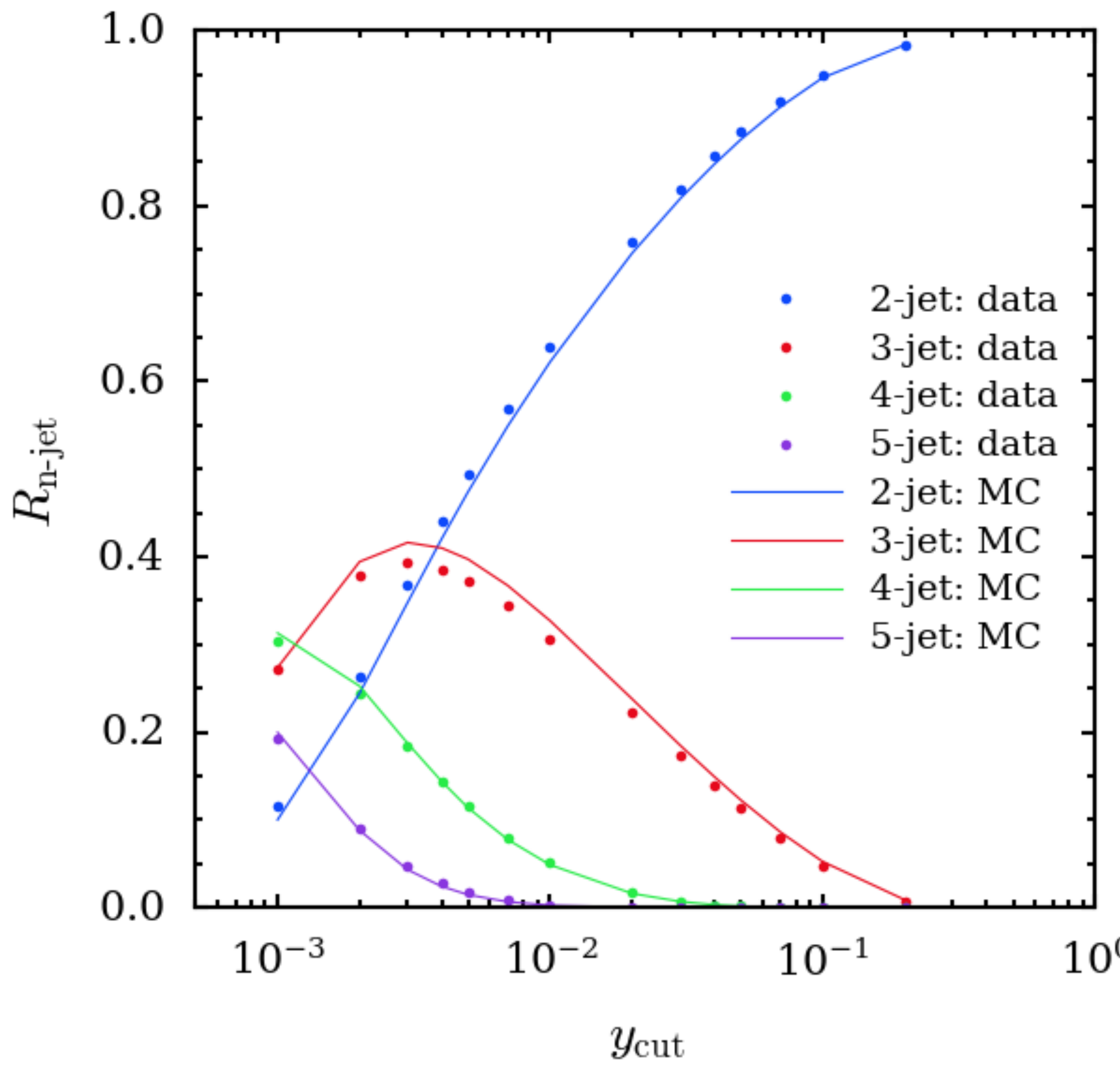

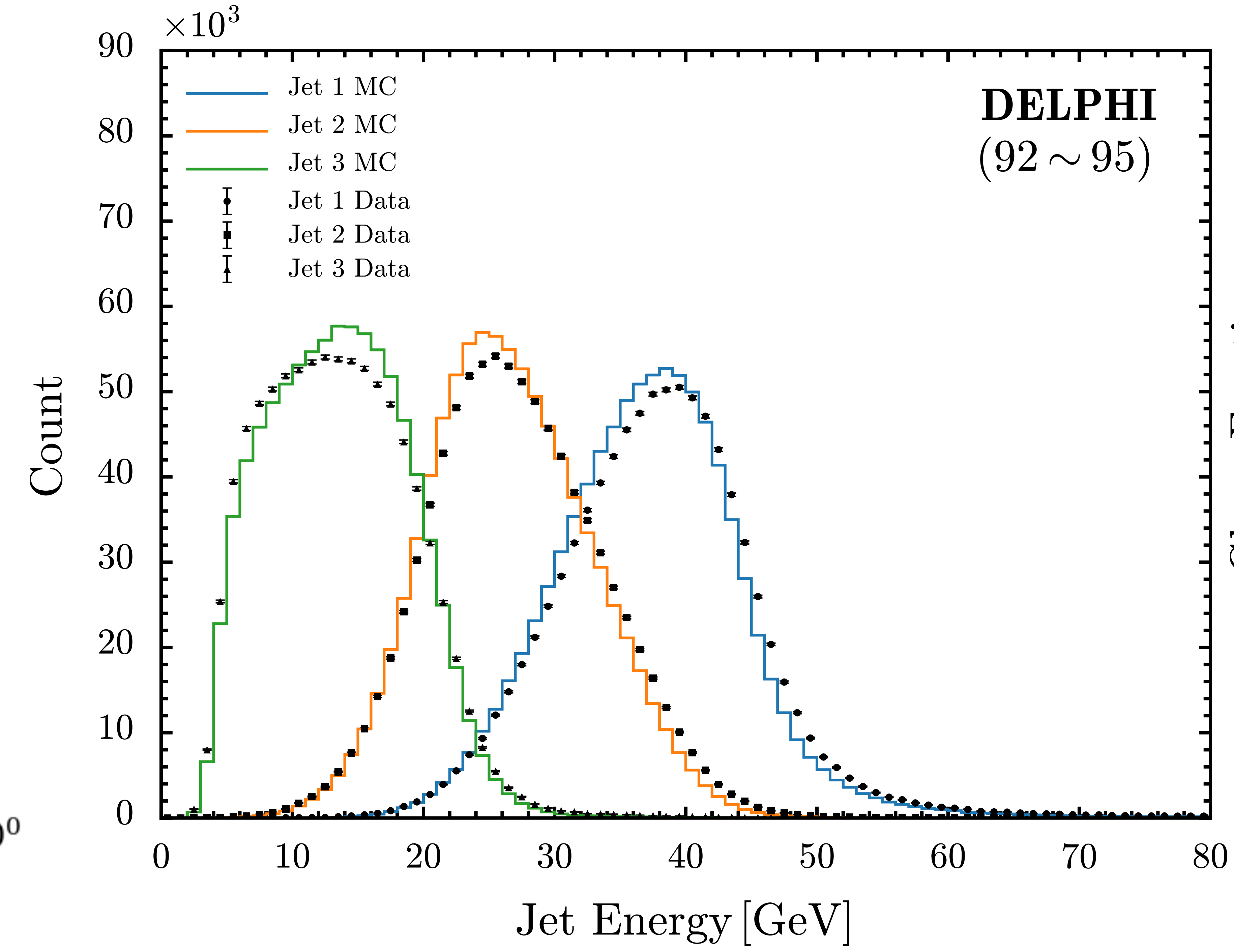

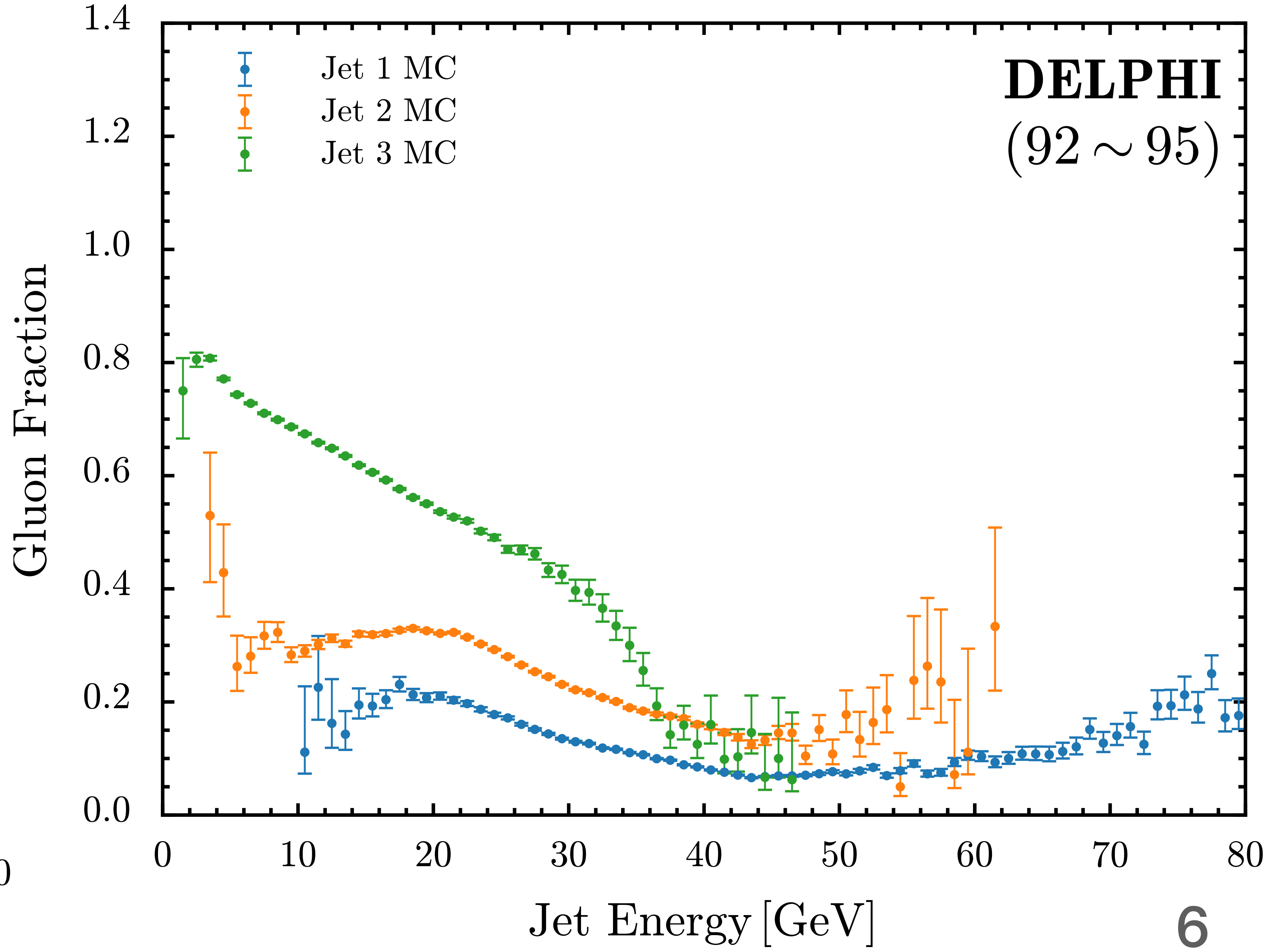

$\Xi^- \to \Lambda + \pi^-$, $\Lambda \to p\pi^-$ Reconstruction

- **Official V^0 selection and our repeat:**
  - All V0's, which means (done by official algorithm, Nucl.Instrum.Meth.A 378 (1996) 57-100):
    - the angle in the xy plane between the V^0 momentum and the line joining the primary to the secondary vertex: $\Delta\phi < 0.1$ rad;
    - the radial separation of the primary and secondary vertex in the XY plane is greater than twice the error on the fitted distance: $R > 2\sigma$;
    - the probability of the χ^2 fit to the secondary vertex: $P_{\chi^2} > 0.001$.
    - $\gamma \to e^+e^-$ veto: the transverse momentum of each particle of the V^0 with respect to the line of flight is greater than $0.02\,\mathrm{GeV}/c$ and the invariant mass in the e^+e^- hypothesis is more than $0.16\,\mathrm{GeV}/c^2$;
  - Considering the tracks with higher momentum as a proton, redo the vertex fit.
  - m_Λ **window:** $|m_{p\pi^-} - m_\Lambda| < 4.5\,\mathrm{MeV}$

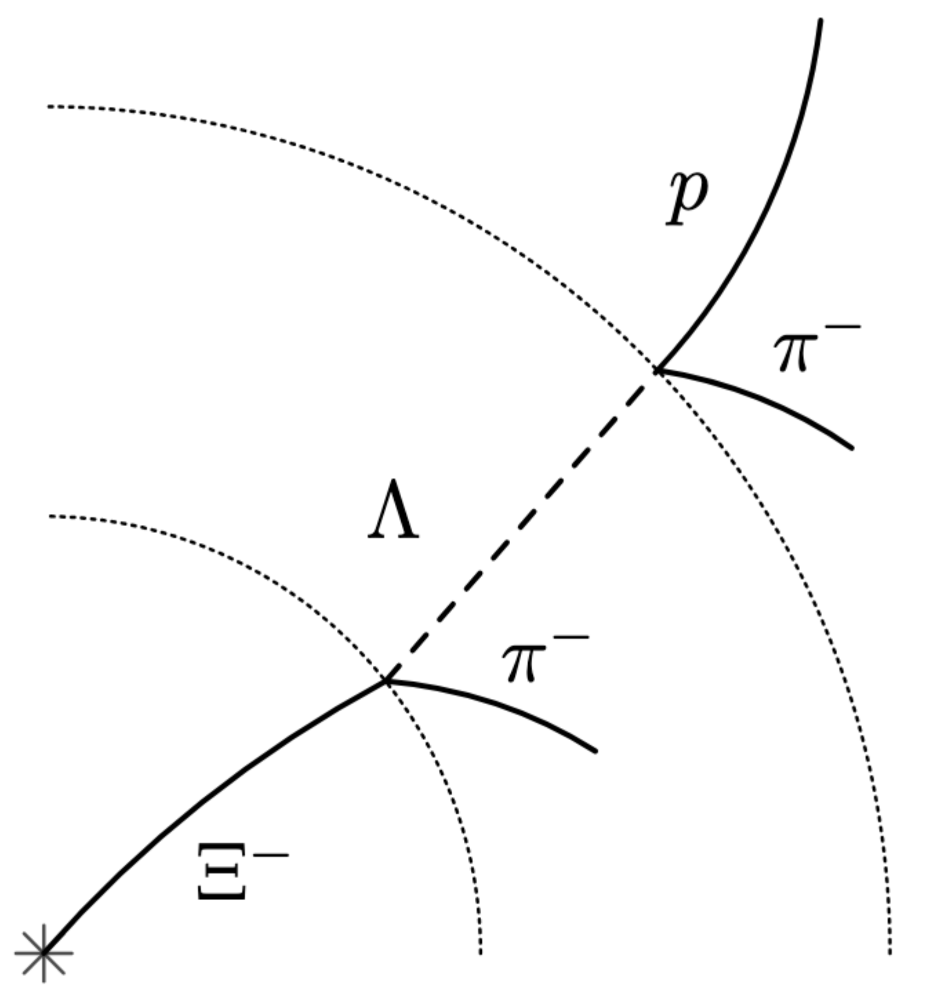

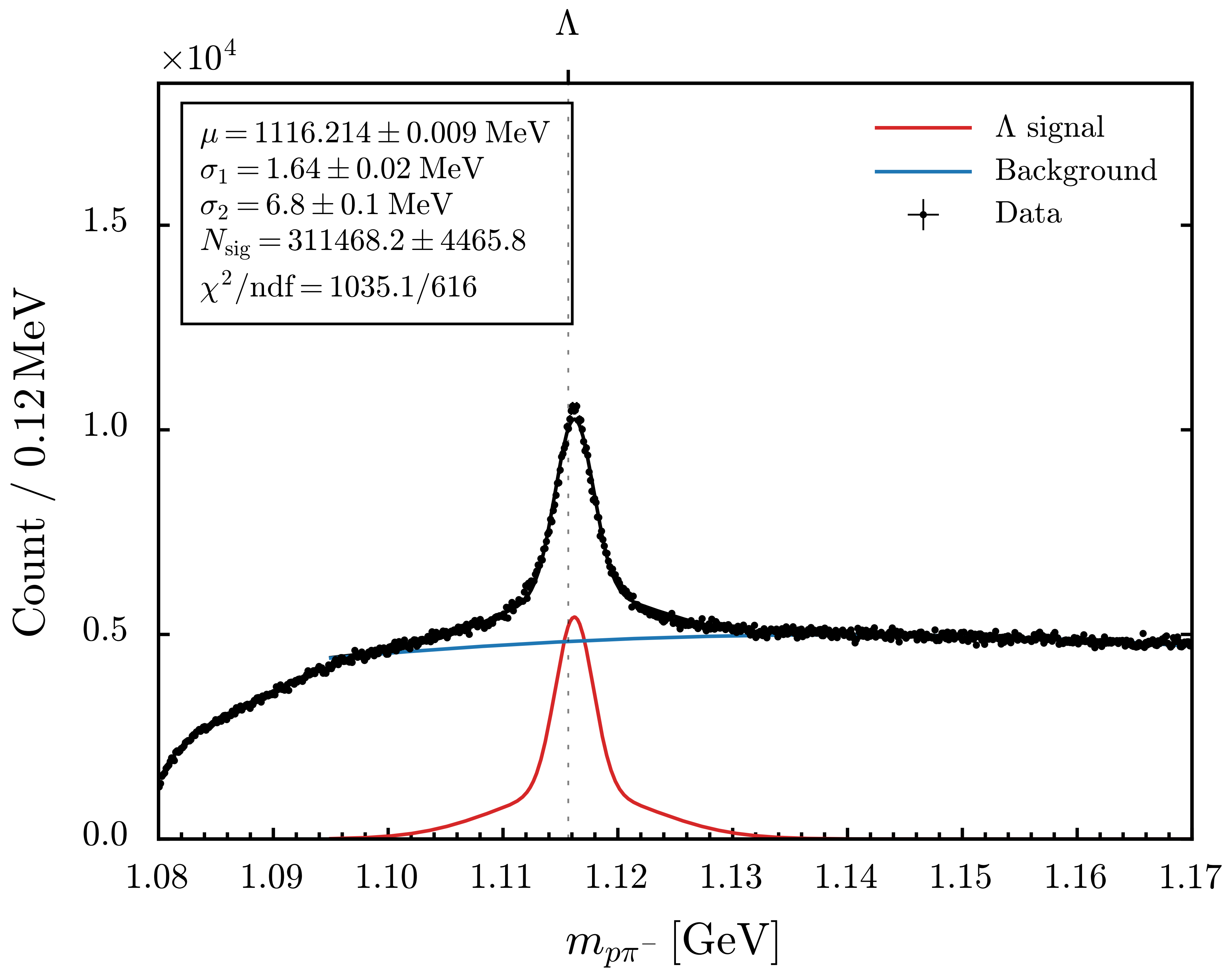

$\Xi^- \to \Lambda + \pi^-$, $\Lambda \to p\pi^-$ Reconstruction

Comparing all the Λ from V0 with the other charged tracks.

- Consider all combinations of $\Lambda + \text{track}^-$ (whose charge is required to be same with π^-_Λ).
- Calculate Ξ^- mass from Λ/Ξ^- VertexFit + Λ KinematicFit.
- A protection cut on probability of $P(\chi^2_{\text{vtx}}) > 0.001$
- Signed decay radius of Ξ^- in $R\phi$ plane: $R_\Xi = \begin{cases} +r_\Xi & \text{if } r_\Lambda > r_\Xi, \\ -r_\Xi & \text{if } r_\Lambda \le r_\Xi, \end{cases} > 0.04\,\text{cm},$

The wrong signed $\Lambda + \text{track}^+$ are considered to model the background.

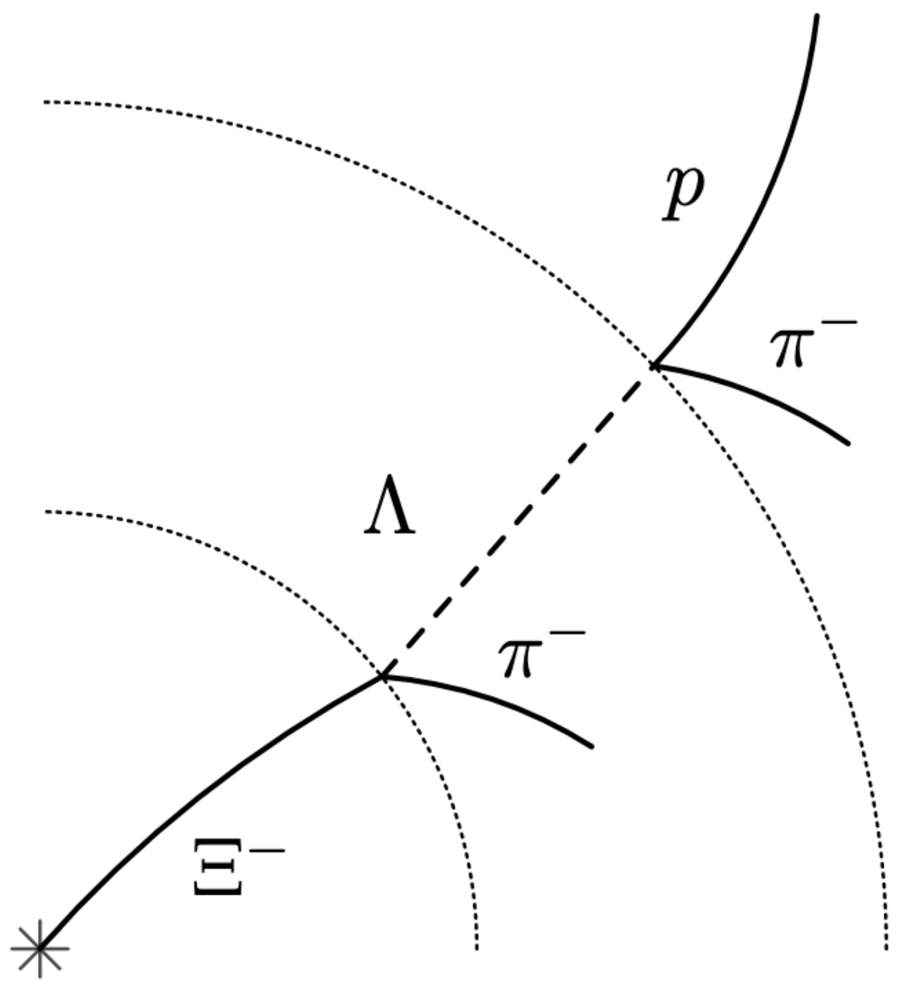

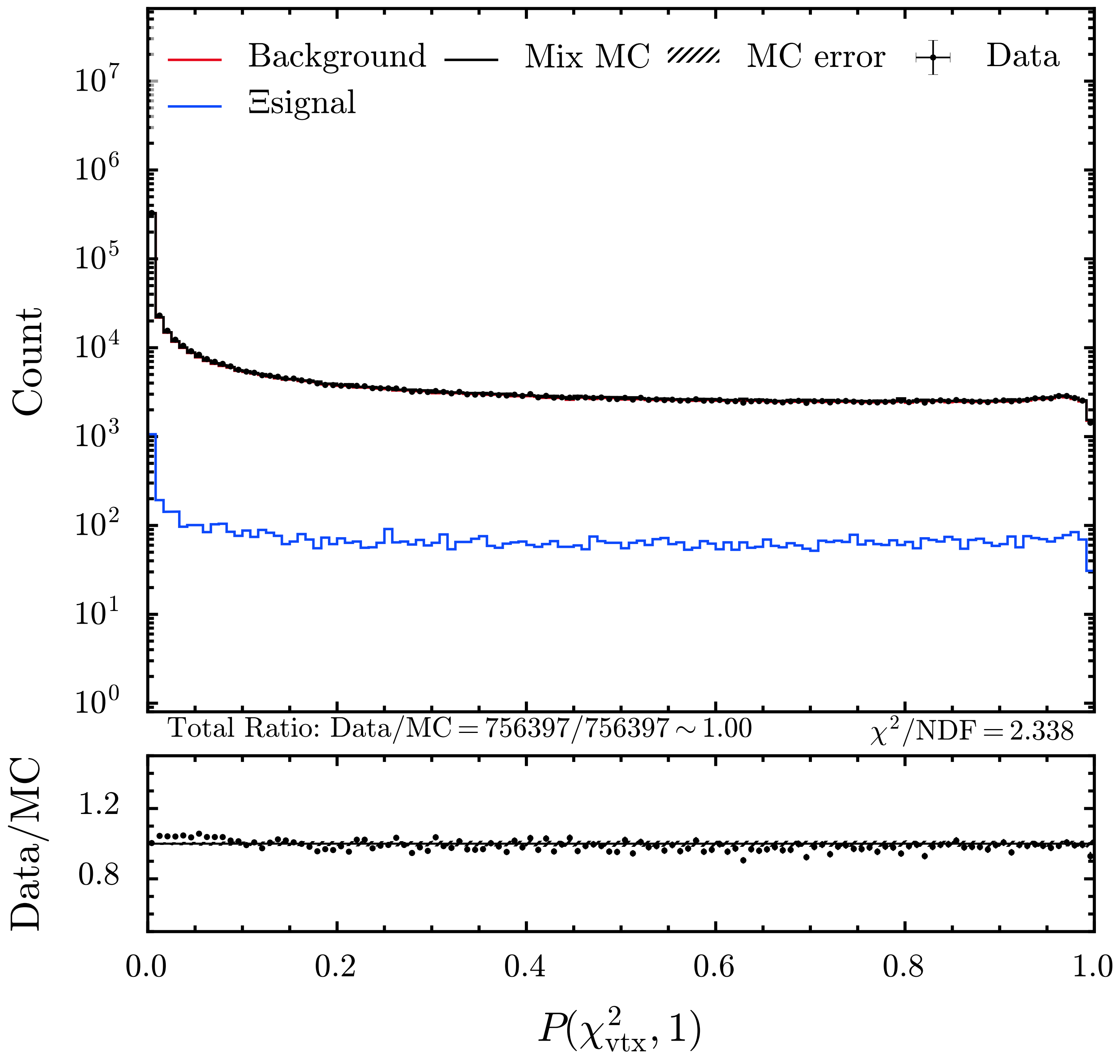

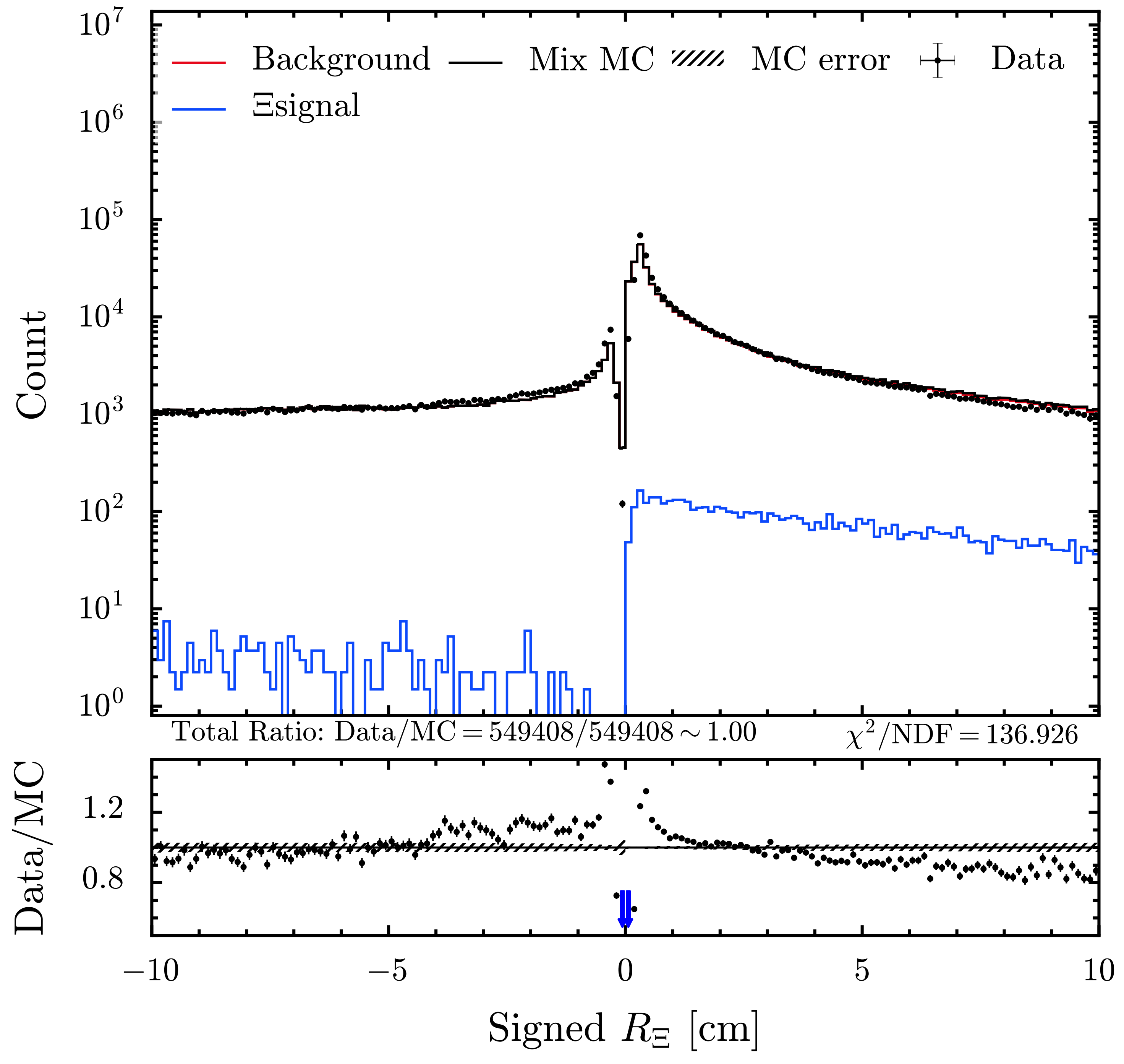

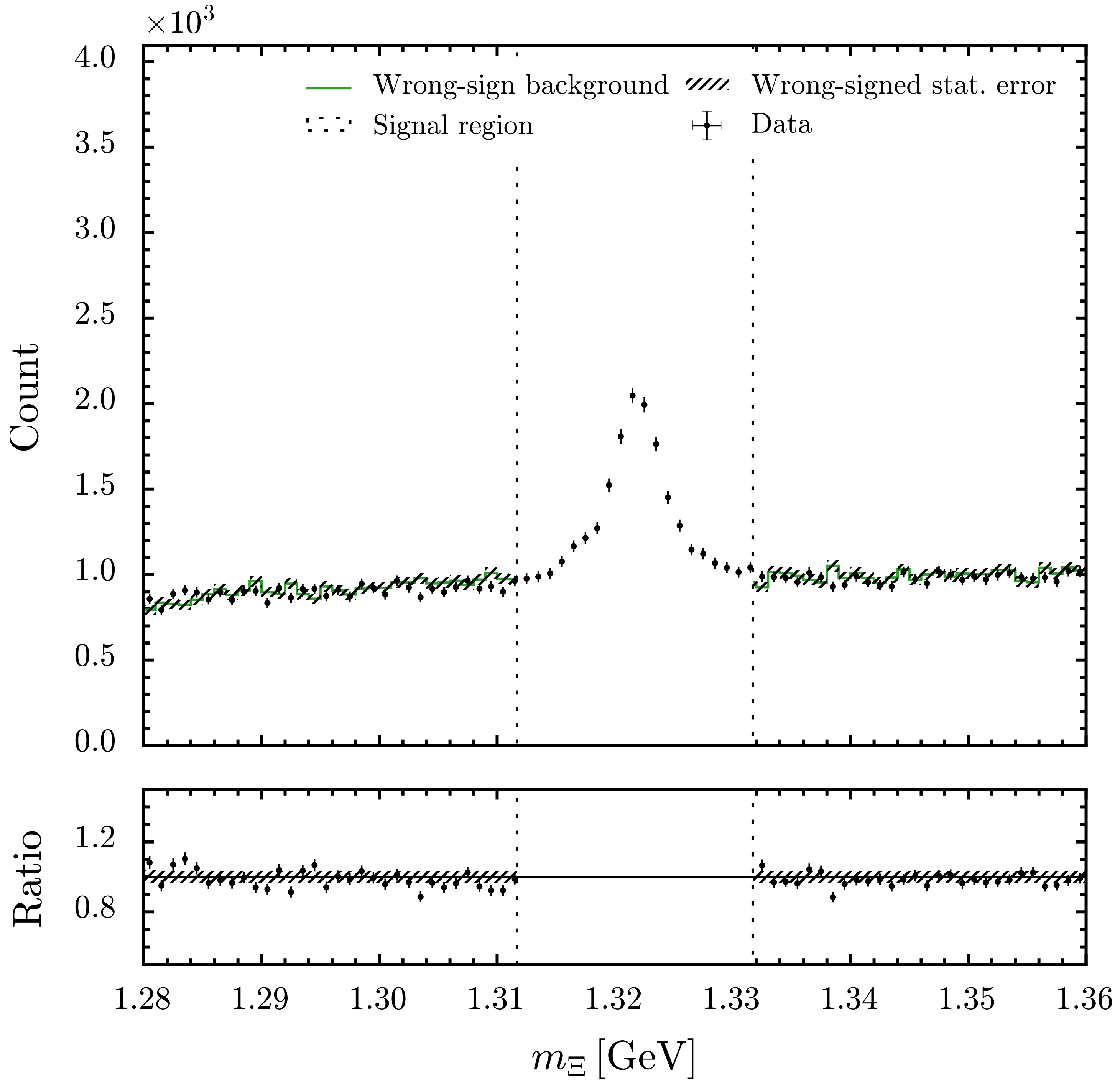

$\Xi^- \to \Lambda + \pi^-$, $\Lambda \to p\pi^-$ Reconstruction

- Selection efficiency of Ξ is studied using truth match between generator particles and reconstructed particles in MC samples

- $$\epsilon_{\text{inc}} = \frac{\text{selected } \Xi \text{ that matched to truth } \Xi}{\text{all truth } \Xi}$$

- DELPHI detector has limited acceptance for $\Xi^- \to \Lambda + \pi^-$, $\Lambda \to p\pi^-$ outside the range of $1.0 < \xi = -\ln p_\Xi / E_{\text{beam}} < 4.0$.

- Only Ξ candidates with $1.0 < \xi = -\ln p_\Xi / E_{\text{beam}} < 4.0$ are considered in the analysis.

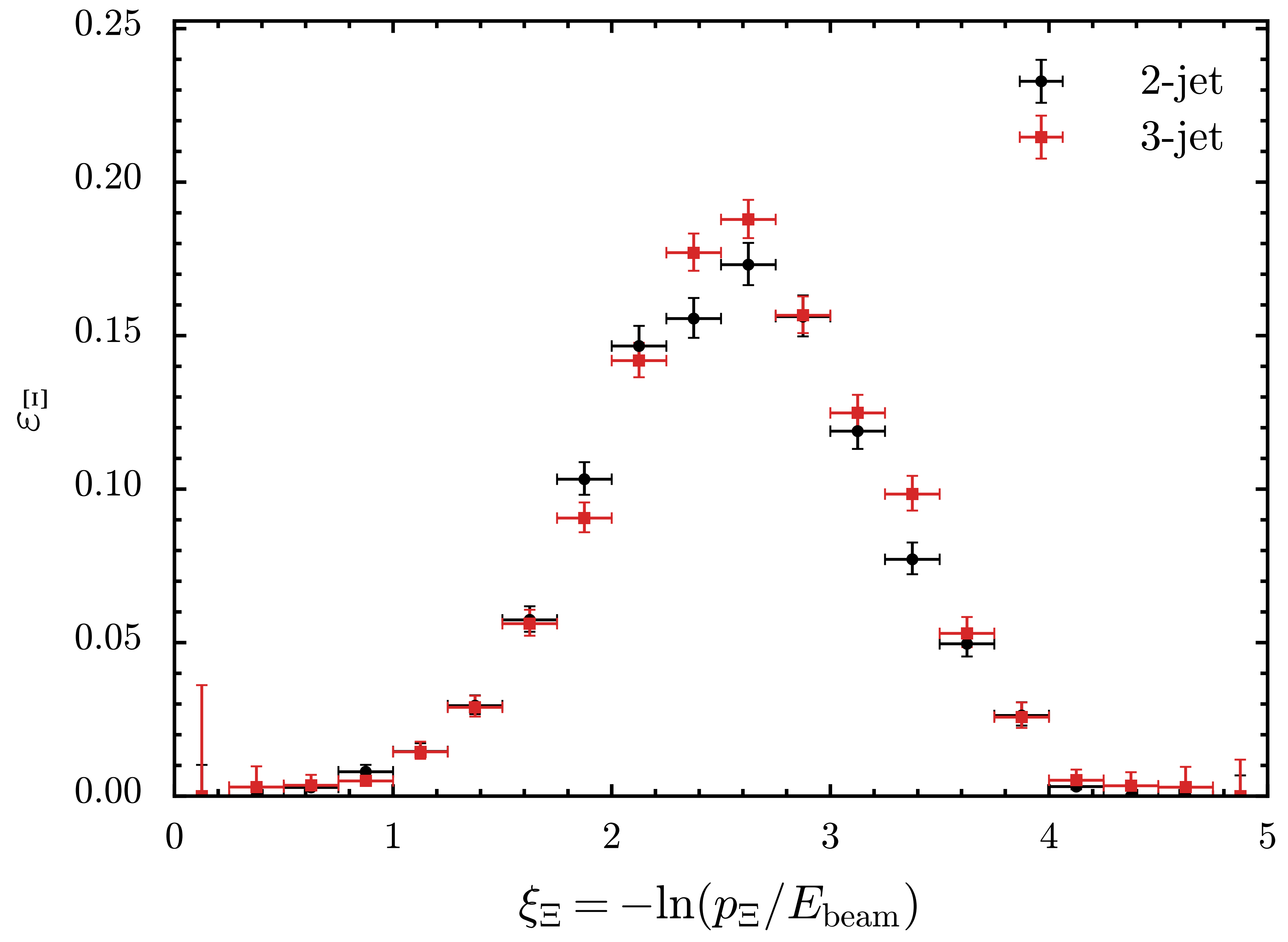

Table 4: Average efficiency of inclusive Ξ^- in 2/3-jet events.

	ε
Inclusive Z	$8.70 \pm 0.08\%$
$Z \to$ 2-Jet Events	$8.14 \pm 0.13\%$
$Z \to$ 3-Jet Events	$10.15 \pm 0.15\%$

Extract Ξ production in jets

- **Ξ-jet assignment:** $y \equiv \dfrac{2 \cdot \min(E_\Xi^2, E_{\rm jet}^2)(1-\cos\theta)}{E_{\rm vis}^2} < 0.005$

- **Extract Ξ production by fitting the Ξ mass spectrum:**
  - PDF: Kernel Density Estimation (KDE) with a Gaussian kernel.
  - Signal modeled by real mass spectrum of MC truth matched Ξ.
  - Background modeled by the wrong signed $\Lambda\pi^+$ pairs from data.

- **Efficiency Correction:**

$$\langle N_\Xi \rangle = \frac{1}{N_{\rm jet}} \frac{N_{\rm obs}}{\epsilon f_{\rm acc}},$$

- ϵ**:** efficiency in acceptance range $1.0 < \xi = -\ln p_\Xi / E_{\rm beam} < 4.0$ and corresponding jets.

- $f_{\rm acc} = \dfrac{N_{\rm gen}(1.0 < \xi < 4.0)}{N_{\rm gen}(\text{full } \xi \text{ range})}$ is estimated from the MC generator.

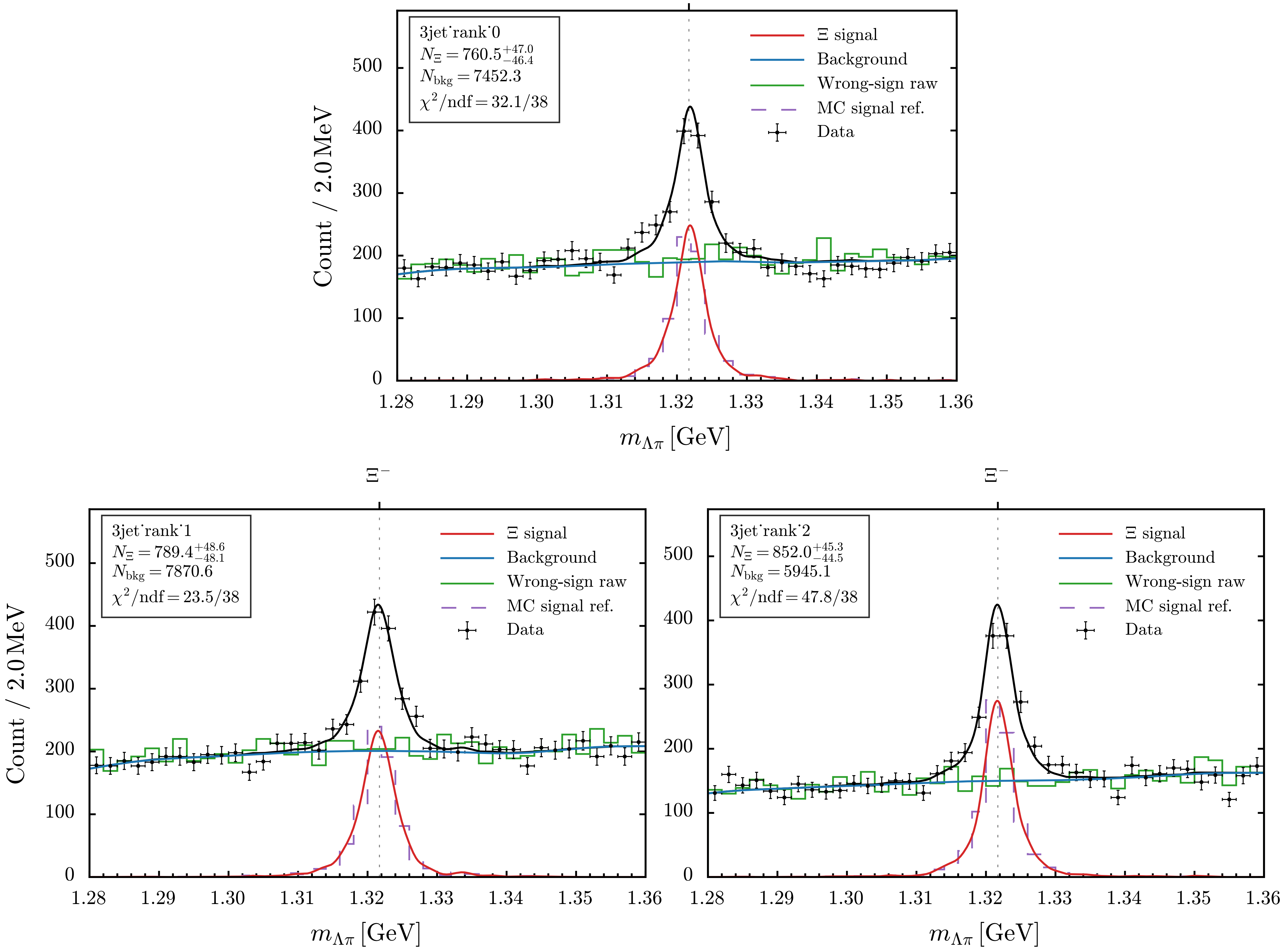

Fit results for Ξ production in energy-ranked jets. Each panel shows the Ξ invariant mass distribution (points) with the KDE signal template (red hatched), background (blue), and total fit (black). The green and purple histograms show the raw distributions of the wrong-signed control sample in data and MC matched Ξ candidates in MC samples.

Systematic uncertainties

- Ξ Selection:
  - m_Λ window: varied from $4.5\,\mathrm{MeV}$ to $4.0\,\mathrm{MeV}$ and $5.0\,\mathrm{MeV}$.
  - minimum signed decay radius of Ξ in $R\phi$-plane: varied from $0.4\,\mathrm{cm}$ to 0, 0.5 and $2.5\,\mathrm{cm}$.
  - Largest variations are considered as the systemtaic uncertainties.
- Fit method:
  - Fit the sideband m_Ξ distribution using histogram PDF of wrong signed control sample, then subtract the background from data in the signal region ($m_\Xi \pm 10\,\mathrm{MeV}$).
  - Half-difference between nominal & alternative fit method is assigned as systematic uncertainty.
- Acceptance:
  - an uncertainty of $50\,\%$ on the correction factor is assigned.

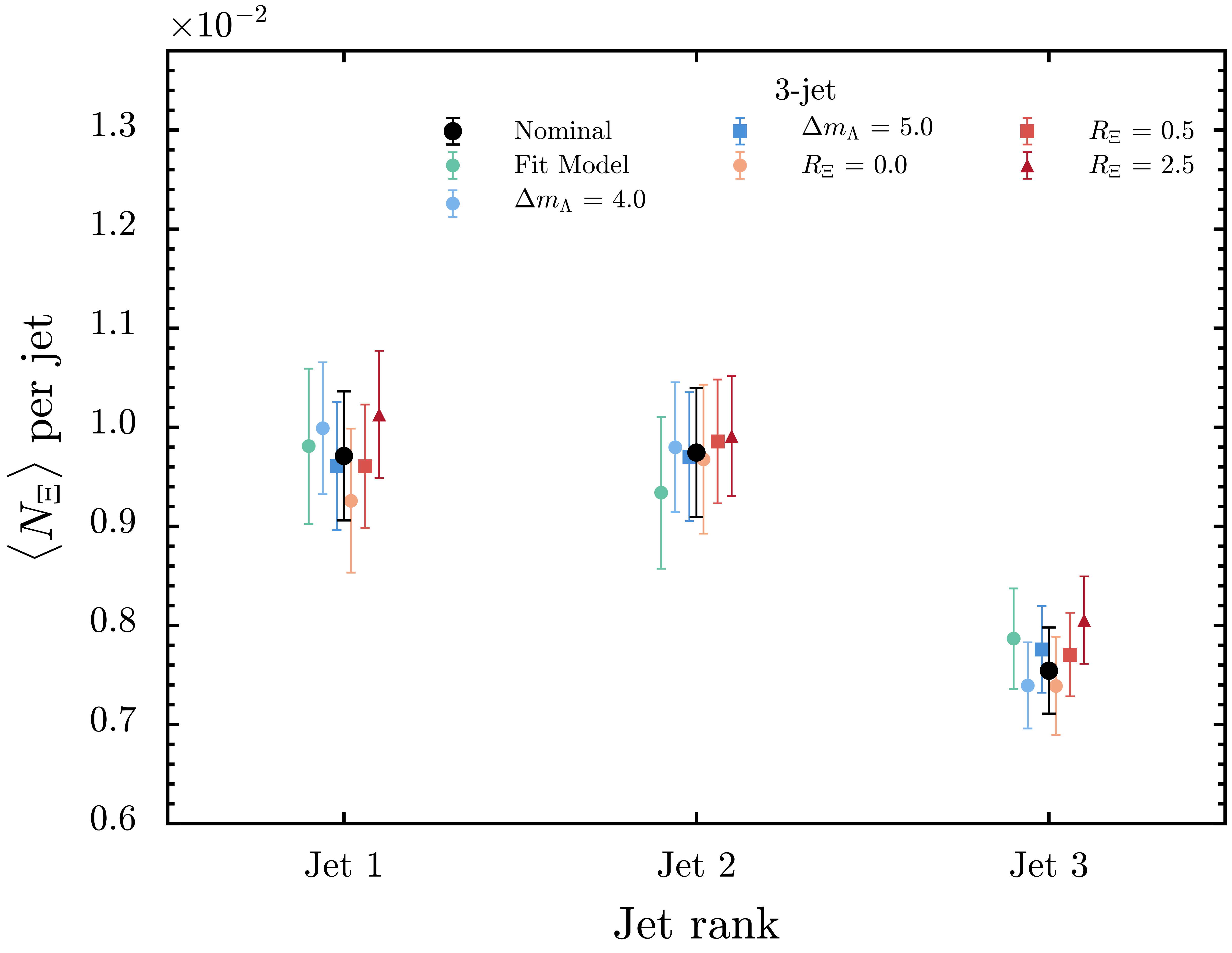

Results

- The resulting average Ξ production in energy ranked jets:

$$\langle N_\Xi \rangle = \frac{1}{N_{\mathrm{jet}}} \frac{N_{\mathrm{obs}}}{\epsilon f_{\mathrm{acc}}},$$

is normalized by the number of inclusive charged tracks in the corresponding jets,

$$R^{\Xi}_{\mathrm{jet},\,k} = \langle N_\Xi \rangle_{\mathrm{jet},\,k} \Big/ \langle N_{\mathrm{ch}} \rangle_{\mathrm{jet},\,k}$$

- The result is compatible with the prediction from the JETSET predictions.

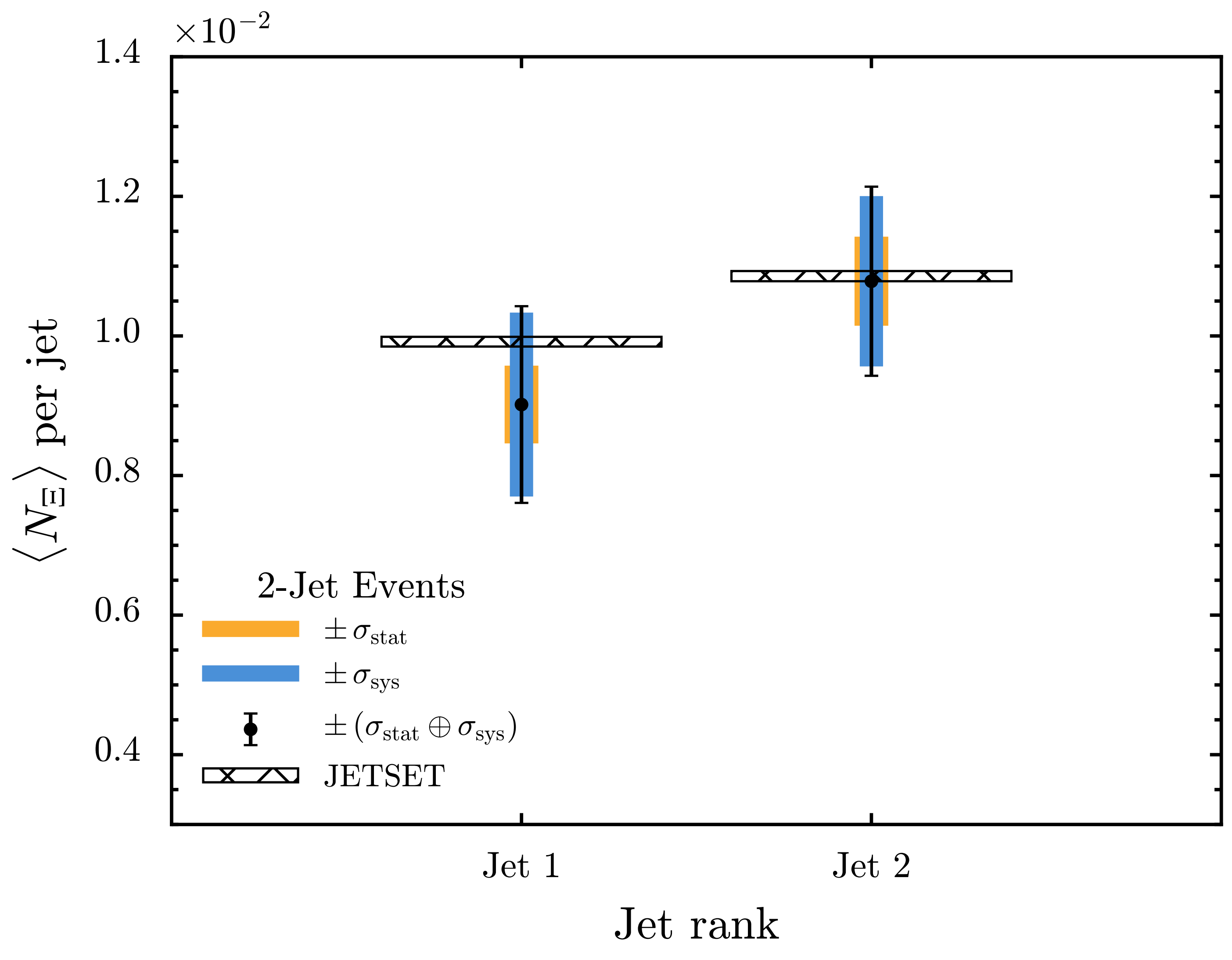

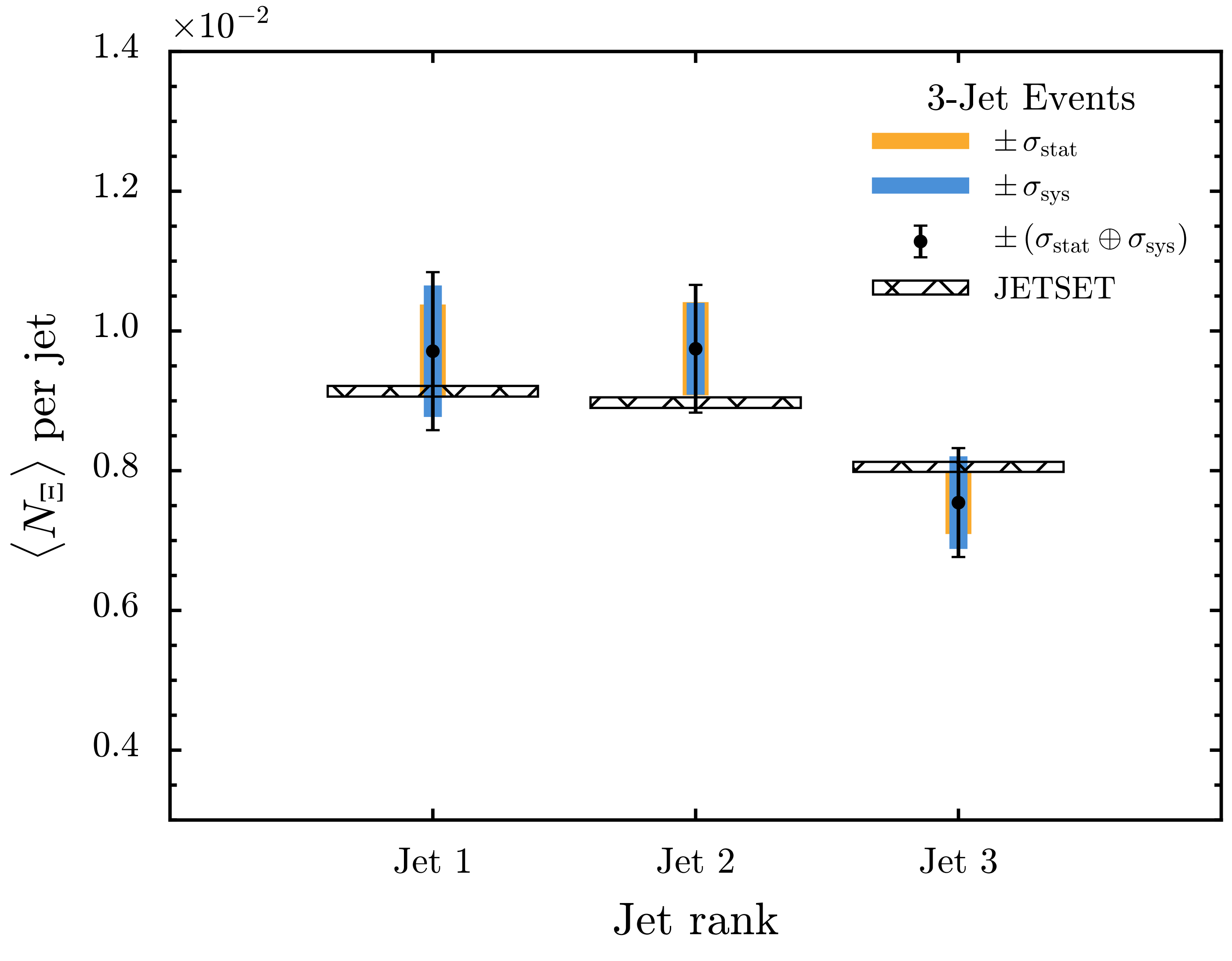

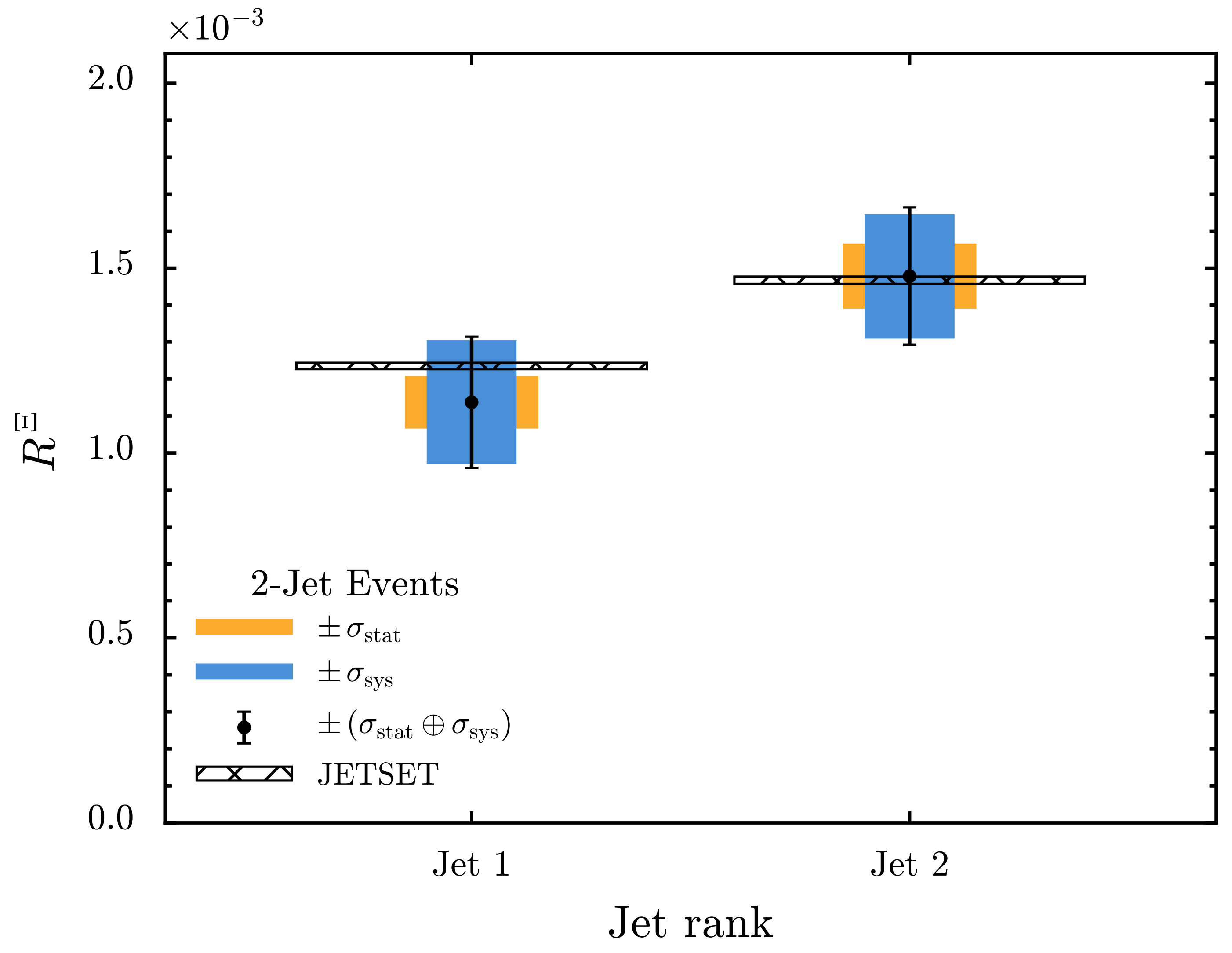

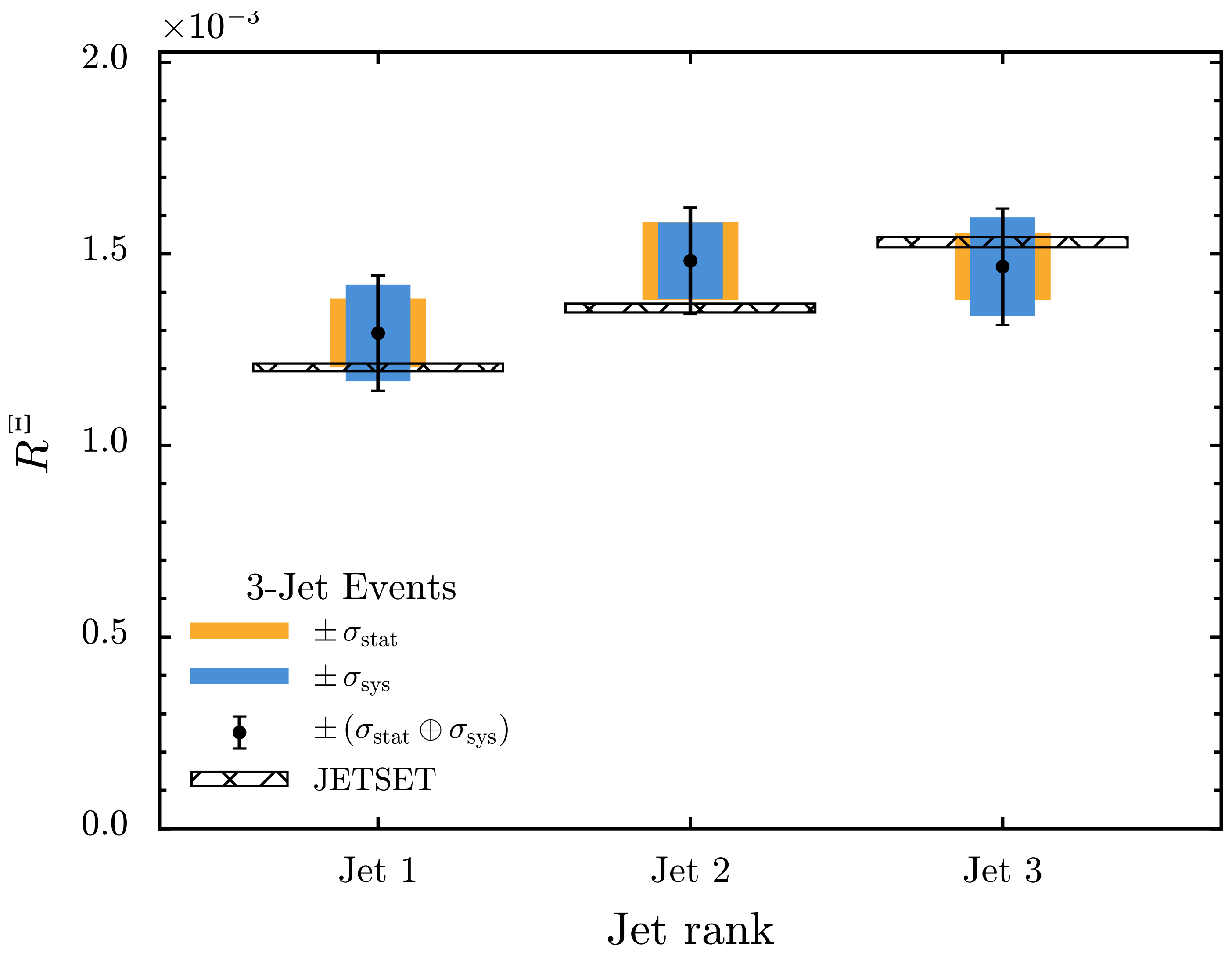

- Production rate ($R^h_{k,\mathrm{obs}}$) of particles in a jet sample (indexed as k) can be considered as a mixture of quark and gluon-jets.

$$R^h_{k,\mathrm{obs}} = \rho_k \cdot R^h_g + (1-\rho_k)\cdot R^h_q,$$

where ρ_k is the gluon-fraction of the jet category. For 3-jet events,

$$\begin{pmatrix} R^h_{1,\mathrm{obs}} \\ R^h_{2,\mathrm{obs}} \\ R^h_{3,\mathrm{obs}} \end{pmatrix} = \begin{pmatrix} 1-\rho_1 & \rho_1 \\ 1-\rho_2 & \rho_2 \\ 1-\rho_3 & \rho_3 \end{pmatrix} \begin{pmatrix} R^h_q \\ R^h_g \end{pmatrix} \equiv A\boldsymbol{\theta}, \quad \boldsymbol{\theta} = \begin{pmatrix} R^h_q \\ R^h_g \end{pmatrix}$$

- Therefore the R^h_q and R^h_g can be derived by a χ^2-fit:

$$\chi^2 = \left(\mathbf{R}_{\mathrm{obs}} - A\boldsymbol{\theta}\right)^T V^{-1} \left(\mathbf{R}_{\mathrm{obs}} - A\boldsymbol{\theta}\right),$$

Then, the ratio $\mathscr{R}^h_{g/q} \equiv \dfrac{\langle N_h\rangle_g}{\langle N_{\mathrm{ch}}\rangle_g} \Big/ \dfrac{\langle N_h\rangle_q}{\langle N_{\mathrm{ch}}\rangle_q}$ can be derived.

The $\mathscr{R}^\Xi_{g/q}$ result is consistent with the ratios of K^0_S and Λ measured by OPAL.

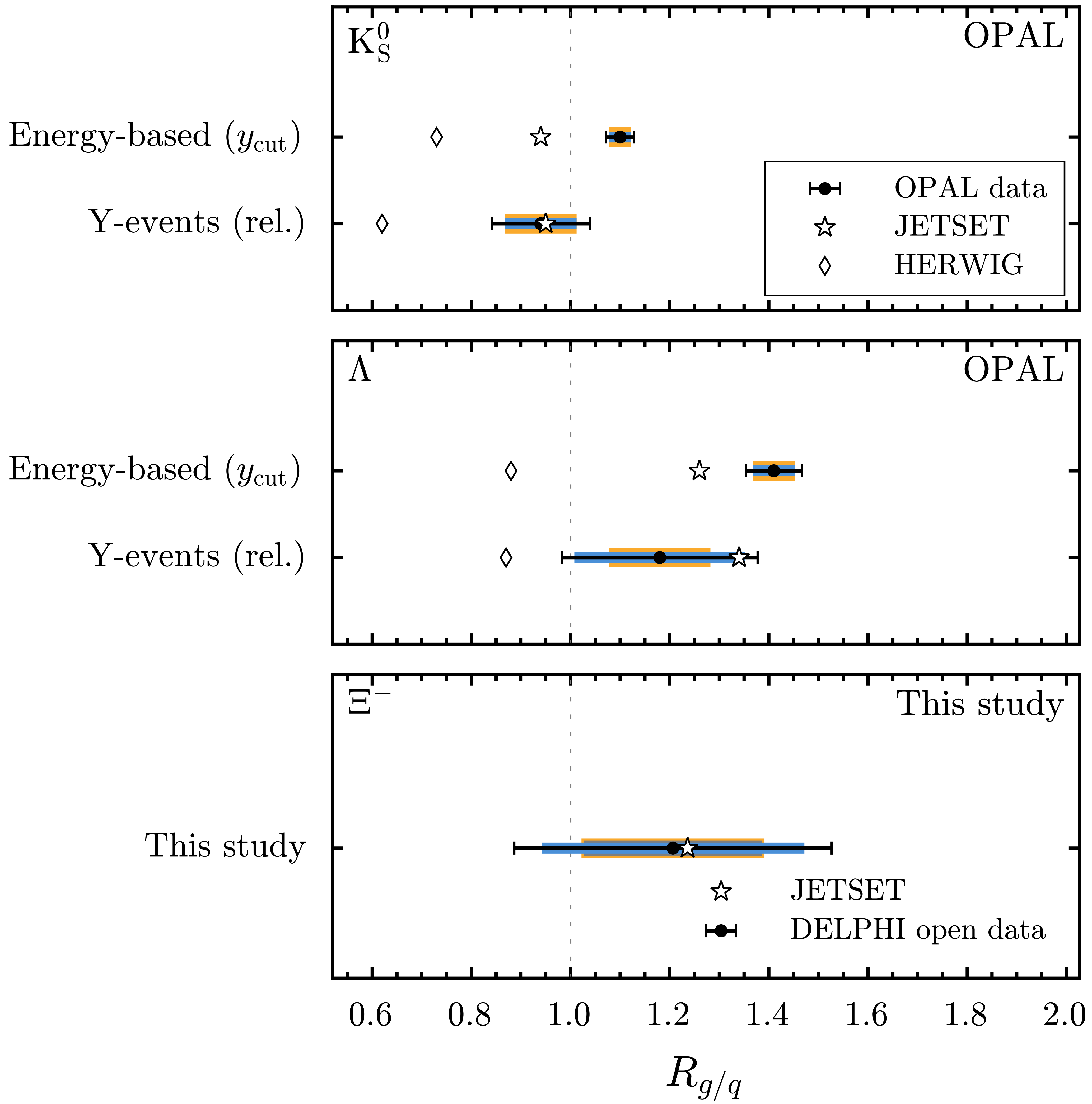

Summary

- This study measures the $\Xi^-/\bar{\Xi}^+$ production rates and momentum spectra in energy-ranked jets using $Z \to \mathrm{hadrons}$ events from the DELPHI open data collected from 1992 to 1995.

- Jets are reconstructed with the Durham algorithm with $y_{\mathrm{cut}} = 0.005$, and quark- and gluon-enriched jet samples are obtained from the energy ordering of jets in three-jet events.

- The average $\Xi^-/\bar{\Xi}^+$ production in energy-ranked jets are measured.

- The ratios of $\Xi^-/\bar{\Xi}^+$ production rates in gluon and quark jets relative to the mean charged particle multiplicity is derived to be

$$R_{gq}^{\Xi} = 1.21 \pm 0.18(\mathrm{stat.}) \pm 0.26(\mathrm{sys.})$$

which is consistent with the JETSET expectation and OPAL result for $\mathscr{R}_{g/q}^{K_S^0}$ and $\mathscr{R}_{g/q}^{\Lambda}$, within the uncertainties.

Thanks for your attention

Back Up

More information

The $\Xi^-/\bar{\Xi}^+$ production in jets as functions of the jet energies, and the $\xi = -\ln(p_\Xi/E_{\text{beam}})$ spectra of $\Xi^-/\bar{\Xi}^+$ in energy ranked jets are also observed to be compatible with the JETSET prediction.

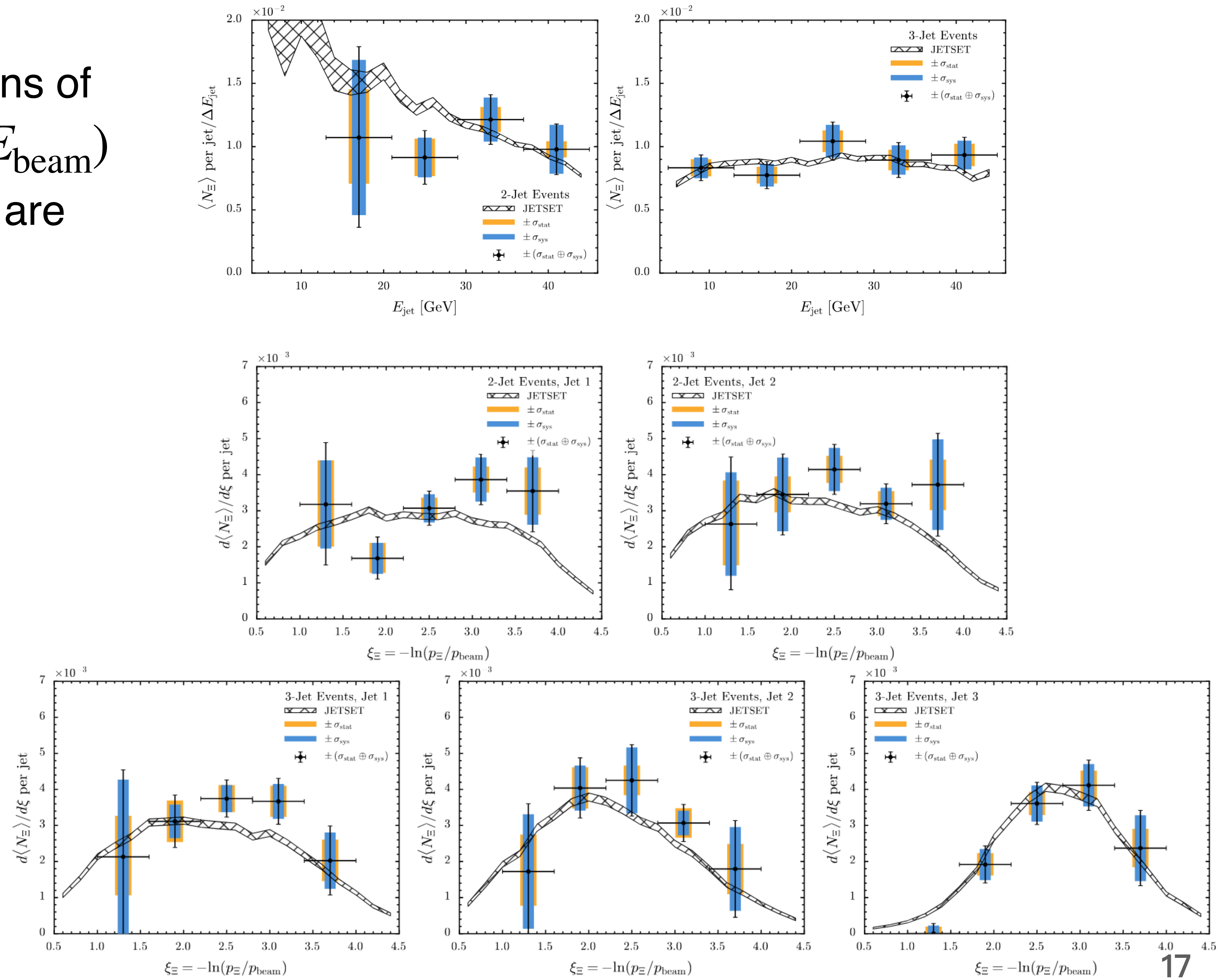

Overview: the Large Electron Positron Collider

The Large Electron-Positron (LEP) collider is **the largest electron-positron accelerator** ever built.

Four detectors on LEP: DELPHI, ALEPH, L3 and OPAL.

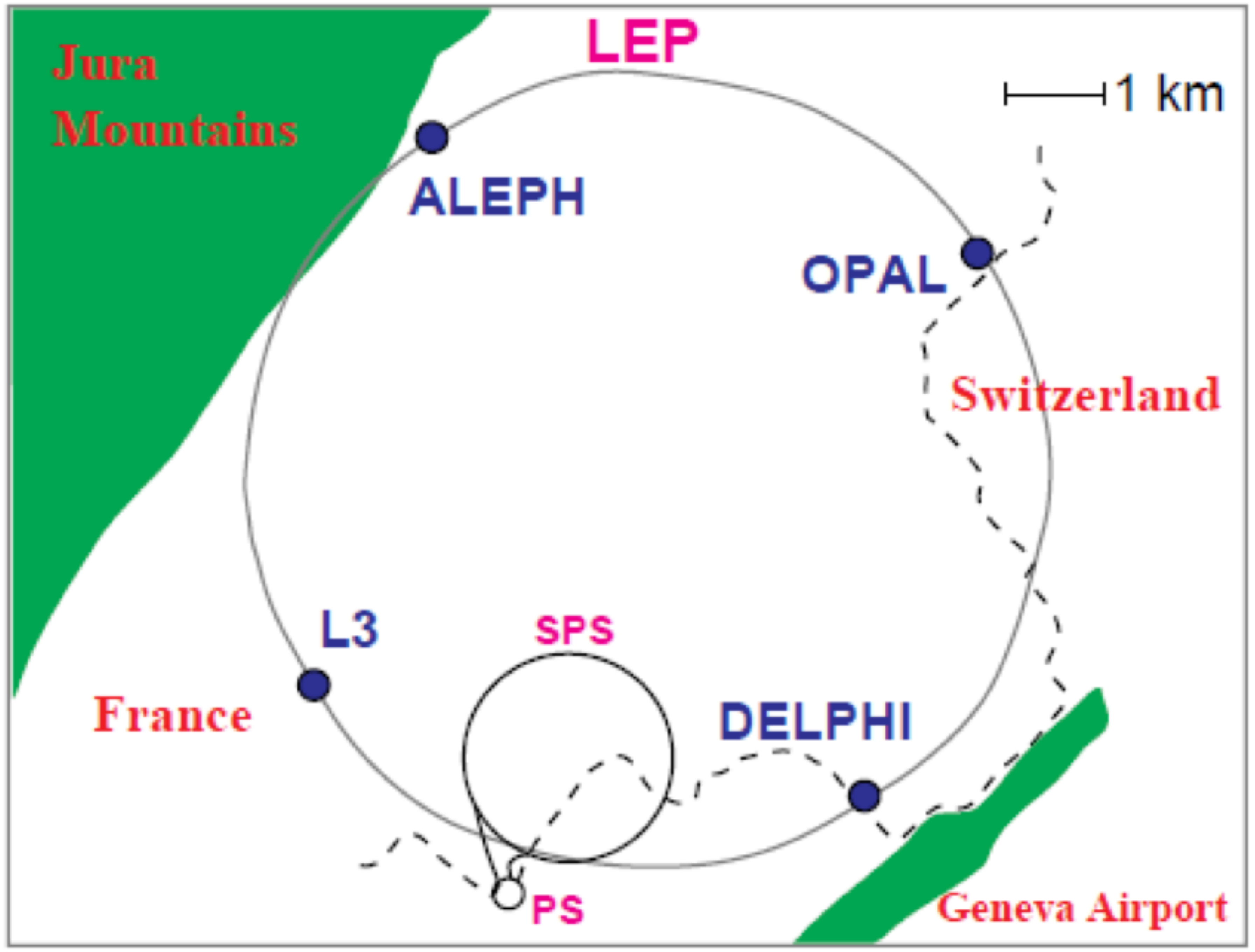

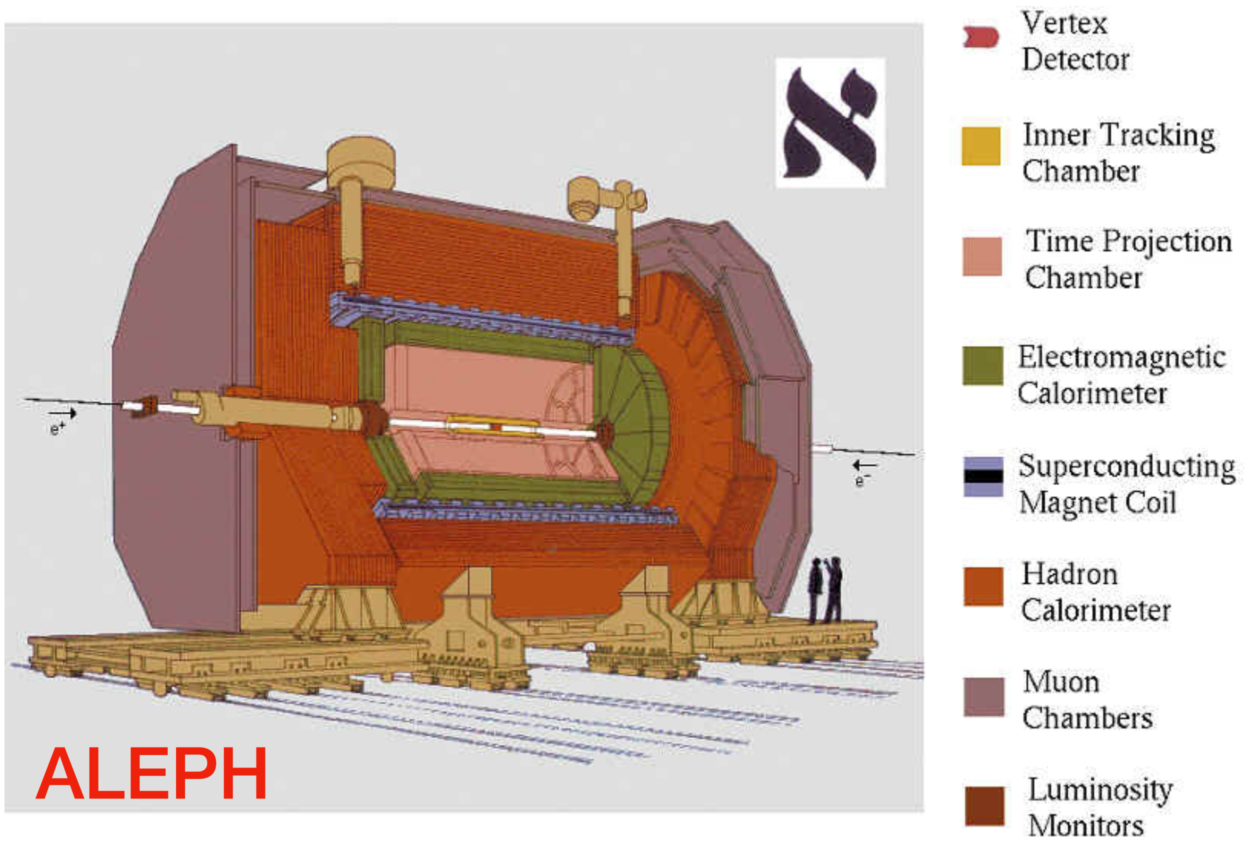

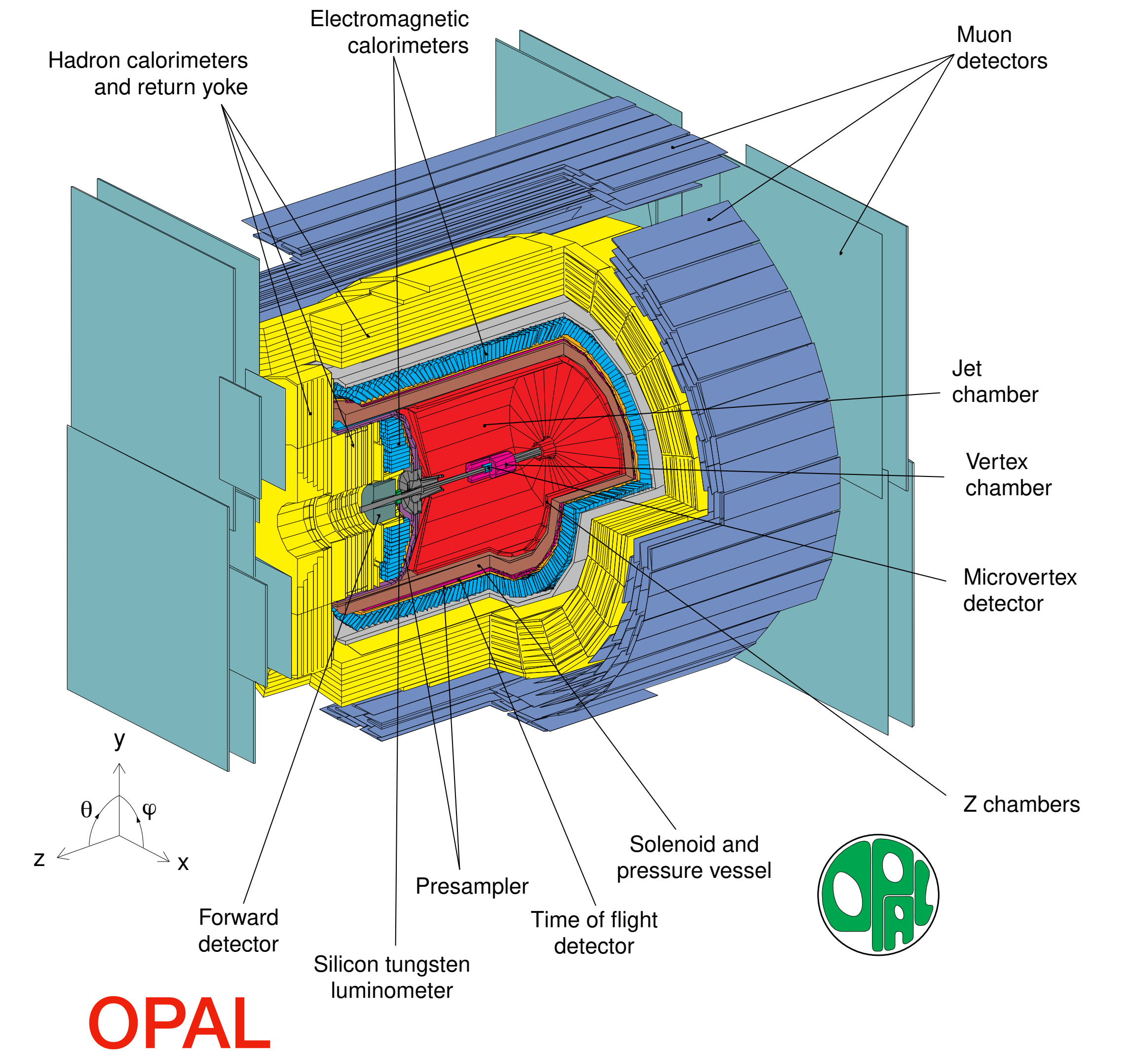

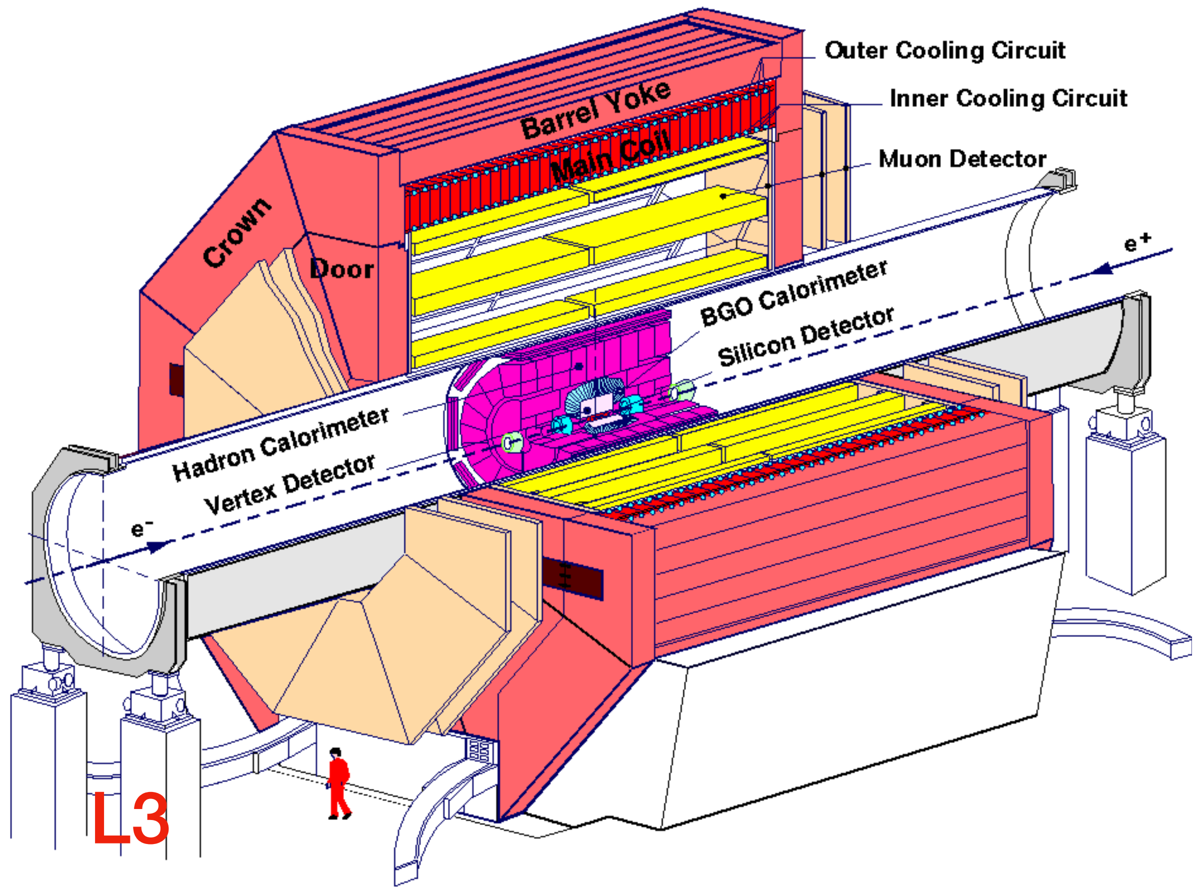

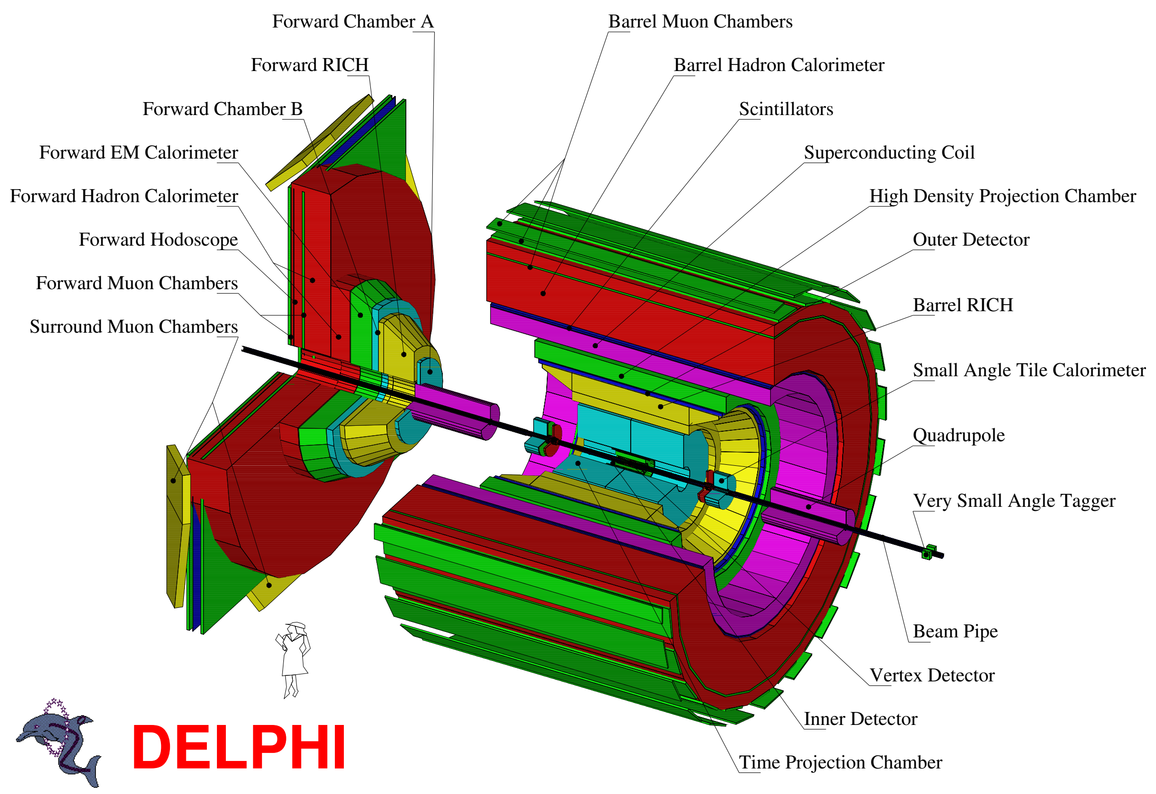

LEP and DELPHI Open Data

The Large Electron-Positron (LEP) collider is **the largest electron-positron accelerator** ever built.

- Two operations from 1990 to 2000:
  LEP I (1990~1995, $91.2\,\mathrm{GeV}$) and **LEP II** (1996~2000, $161\text{~}205\,\mathrm{GeV}$).
- The LEP terminated in 2000, and the collaboration activity continued till 2017

Four detectors on LEP: **DELPHI**, ALEPH, L3 and OPAL.

In 2024, the DELPHI collaboration decided to open the data and original software stack to the physics community **for public access** (see *DELPHI data preservation, re-use, and open access policy*) :

- original DELPHI analysis framework
- simulation & reconstruction
- the event display
- and documentation.

Other experiments' datasets are archived on EOS awaiting similar release (see *4th DPHEP Collaboration Workshop*).

Number of Events										
	$Z \to q\bar{q}$					$Z \to \ell^+\ell^-$				
Year	A	D	L	O	LEP	A	D	L	O	LEP
1990/91	433	357	416	454	1660	53	36	39	58	186
1992	633	697	678	733	2741	77	70	59	88	294
1993	630	682	646	649	2607	78	75	64	79	296
1994	1640	1310	1359	1601	5910	202	137	127	191	657
1995	735	659	526	659	2579	90	66	54	81	291
Total	4071	3705	3625	4096	15497	500	384	343	497	1724

Table 1.2: The $q\bar{q}$ and $\ell^+\ell^-$ event statistics, in units of 10^3, used for Z analyses by the experiments ALEPH (A), DELPHI (D), L3 (L) and OPAL (O).

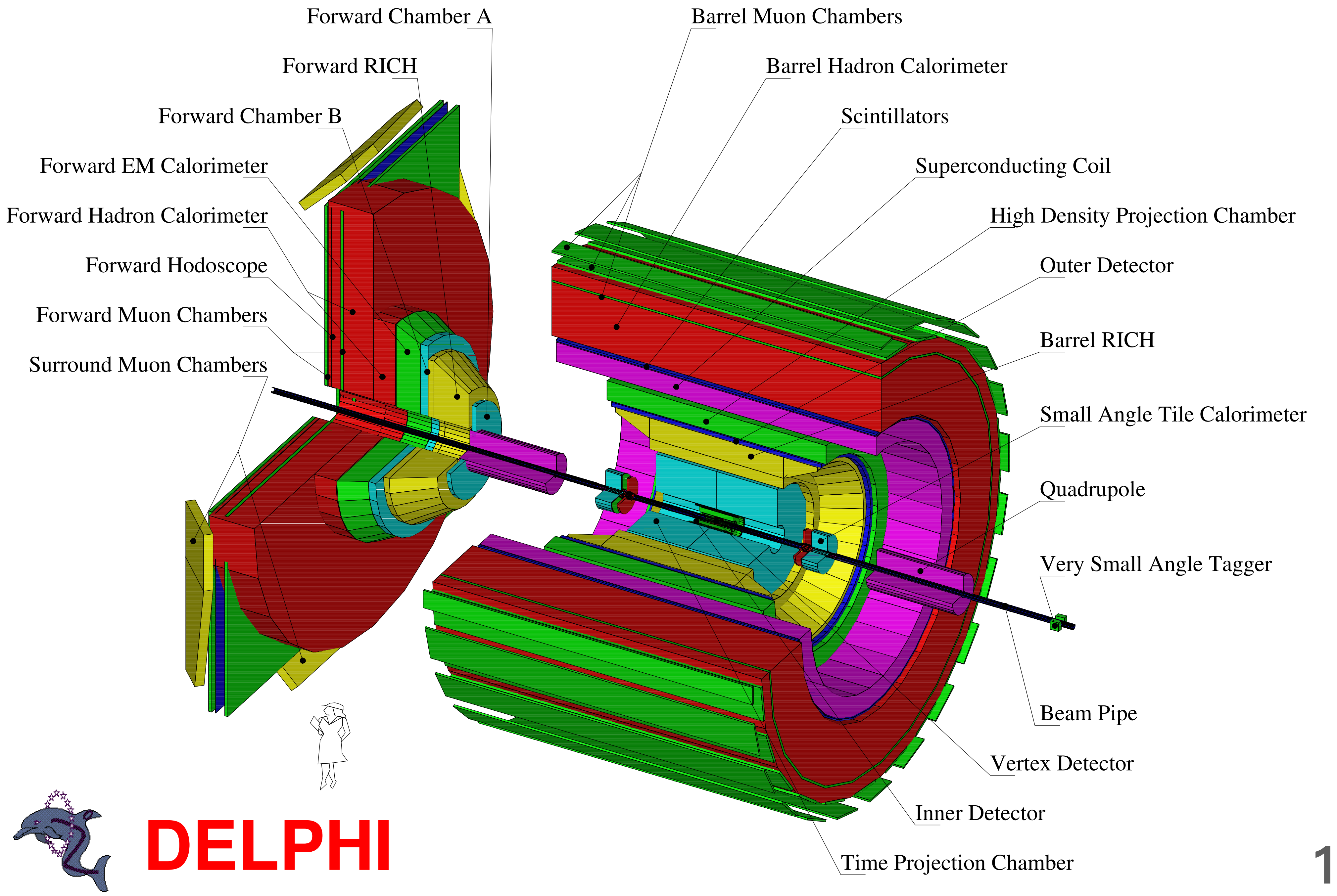

Numerical Result: $\langle N_\Xi \rangle$ in Energy Ranked Jets

TABLE II. Average Ξ production per jet in 2- and 3-jet events. The central observable is computed as $\langle N_\Xi \rangle = N_{\rm obs}/(\epsilon f_{\rm acc} N_{\rm jet})$ from the fitted signal yield ($N_{\rm obs}$), selection efficiency (ϵ), acceptance factor ($f_{\rm acc}$, and the number of jets ($N_{\rm jet}$. Relative statistical ($\sigma_{\rm stat}$) and systematic ($\sigma^{\rm tot}_{\rm syst}$) uncertainties on $\langle N_\Xi \rangle$ are listed in percentage, with $\sigma^{\rm tot}_{\rm syst}$ divided in the contributions from the cut on Λ mass (Δm_Λ), signed Ξ^- decay radius in $R\phi$ plane (R_Ξ), Fit method extracting the signal yield (Fit) and the acceptance correction (Acc.). The uncertainties are added in quadrature as the total uncertainty ($\sigma_{\rm total}$) listed in the last column.

Jet Num.	Jet Rank	$N_{\rm obs}$	ϵ [%]	$f_{\rm acc}$ [%]	$N_{\rm jet}$	$\langle N_\Xi \rangle$ $\times 10^{-3}$	$\sigma_{\rm stat}$ [%]	$\sigma_{\rm syst}$ Δm_Λ	R_Ξ	Fit	Acc.	$\sigma_{\rm syst}$ [%]	$\sigma_{\rm total}$ [%]
2-jet	Jet 1	977.4	10.8	79.9	1 259 717	9.0	$^{+6.0}_{-6.0}$	2.3	9.4	3.7	10.0	14.4	$^{+15.6}_{-15.6}$
2-jet	Jet 2	1031.6	9.4	80.6	1 259 717	10.8	$^{+5.8}_{-5.8}$	2.8	4.8	0.4	9.7	11.2	$^{+12.6}_{-12.6}$
3-jet	Jet 1	760.5	10.4	84.5	889 570	9.7	$^{+6.7}_{-6.7}$	2.9	4.7	0.5	7.8	9.5	$^{+11.7}_{-11.6}$
3-jet	Jet 2	789.4	10.3	88.0	889 570	9.7	$^{+6.7}_{-6.7}$	0.5	1.7	2.1	6.0	6.6	$^{+9.4}_{-9.4}$
3-jet	Jet 3	852.0	13.8	92.2	889 570	7.5	$^{+5.8}_{-5.7}$	2.8	6.8	2.1	3.9	8.6	$^{+10.3}_{-10.3}$

Numerical Result: $\langle N_\Xi \rangle$ vs E_{jet}

TABLE III. Average Ξ production per accepted jet as a function of reconstructed jet energy, computed in each energy bin as $\langle N_\Xi \rangle = N_{\mathrm{obs}}/(\epsilon f_{\mathrm{acc}} N_{\mathrm{jet}})$. Relative statistical ($\sigma_{\mathrm{stat}}$) and systematic ($\sigma_{\mathrm{syst}}^{\mathrm{tot}}$) uncertainties on $\langle N_\Xi \rangle$ are listed in percentage, with $\sigma_{\mathrm{syst}}^{\mathrm{tot}}$ divided in the contributions from the cut on Λ mass (Δm_Λ), signed Ξ^- decay radius in $R\phi$ plane (R_Ξ), Fit method extracting the signal yield (Fit) and the acceptance correction (Acc.). The uncertainties are added in quadrature as the total uncertainty (σ_{total}) listed in the last column.

Jet Num.	E_{Jet} [GeV] min − max	N_{obs}	ϵ [%]	f_{acc} [%]	N_{jet}	$\langle N_\Xi \rangle$ $\times 10^{-3}$	σ_{stat} [%]	σ_{syst}[%] Δm_Λ	R_Ξ	Fit	Acc.	$\sigma_{\mathrm{syst}}^{\mathrm{tot}}$ [%]	σ_{total} [%]
2-jet	5.0 – 13.0	0.0	5.4	47.4	8881	< 42.2	–	–	–	–	–	–	–
2-jet	13.0 – 21.0	29.5	7.0	67.0	58 733	10.7	$^{+35.3}_{-33.8}$	15.2	39.5	34.4	16.5	57.0	$^{+67.0}_{-66.2}$
2-jet	21.0 – 29.0	132.9	8.0	77.6	235 364	9.1	$^{+16.0}_{-15.7}$	9.0	7.8	4.3	11.2	16.9	$^{+23.3}_{-23.1}$
2-jet	29.0 – 37.0	539.2	9.0	82.7	598 031	12.1	$^{+7.9}_{-7.9}$	2.6	10.6	2.4	8.7	14.1	$^{+16.2}_{-16.2}$
2-jet	37.0 – 45.0	880.4	11.3	82.4	966 668	9.8	$^{+6.3}_{-6.3}$	0.4	17.3	1.6	8.8	19.5	$^{+20.4}_{-20.4}$
3-jet	5.0 – 13.0	412.5	13.4	90.9	406 731	8.3	$^{+7.8}_{-7.8}$	2.1	5.4	5.8	4.6	9.4	$^{+12.2}_{-12.2}$
3-jet	13.0 – 21.0	474.0	12.8	90.1	530 483	7.7	$^{+8.2}_{-8.1}$	4.2	9.0	1.3	5.0	11.2	$^{+13.9}_{-13.8}$
3-jet	21.0 – 29.0	534.3	10.1	88.8	573 428	10.4	$^{+8.0}_{-8.0}$	0.1	8.5	6.6	5.6	12.1	$^{+14.5}_{-14.5}$
3-jet	29.0 – 37.0	472.4	10.7	87.4	563 681	8.9	$^{+8.9}_{-8.8}$	3.6	10.0	2.7	6.3	12.6	$^{+15.4}_{-15.4}$
3-jet	37.0 – 45.0	402.6	12.1	84.4	422 890	9.3	$^{+9.2}_{-9.2}$	3.1	6.7	5.0	7.8	11.8	$^{+15.0}_{-15.0}$

Numerical Result: ξ spectrum of $\Xi^-/\bar{\Xi}^+$

TABLE IV. Differential Ξ production per accepted jet versus $\xi_\Xi = -\ln(p_\Xi/p_{\mathrm{beam}})$, grouped by topology and jet rank. Because this spectrum is measured inside the accepted ξ range, no global f_{acc} factor is applied; the central value is $\mathrm{d}\langle N_\Xi\rangle/\mathrm{d}\xi = N_{\mathrm{obs}}/(\epsilon N_{\mathrm{jet}}\Delta\xi)$. Relative statistical ($\sigma_{\mathrm{stat}}$) and systematic ($\sigma^{\mathrm{tot}}_{\mathrm{syst}}$) uncertainties on $\langle N_\Xi\rangle$ are listed in percentage, with $\sigma^{\mathrm{tot}}_{\mathrm{syst}}$ divided in the contributions from the cut on Λ mass (Δm_Λ), signed Ξ^- decay radius in $R\phi$ plane (R_Ξ), and Fit method extracting the signal yield (Fit). The uncertainties are added in quadrature as the total uncertainty (σ_{total}) listed in the last column.

Jet Num.	Jet Rank	ξ_Ξ min – max	N_{obs}	ϵ [%]	N_{jet}	$\mathrm{d}\langle N_\Xi\rangle/\mathrm{d}\xi$ $\times 10^{-3}$	σ_{stat} [%]	σ_{syst}[%] Δm_Λ	R_Ξ	Fit	$\sigma^{\mathrm{tot}}_{\mathrm{syst}}$ [%]	σ_{total} [%]
2-jet	Jet 1	1.0 – 1.6	60.5	3.2	1 259 717	2.54	$^{+38.1}_{-36.6}$	21.4	29.9	2.5	36.9	$^{+53.0}_{-51.9}$
2-jet	Jet 1	1.6 – 2.2	118.8	11.7	1 259 717	1.34	$^{+25.0}_{-23.5}$	14.0	17.5	5.3	23.1	$^{+34.0}_{-32.9}$
2-jet	Jet 1	2.2 – 2.8	354.0	19.1	1 259 717	2.45	$^{+9.3}_{-9.2}$	4.1	5.8	1.9	7.4	$^{+11.9}_{-11.8}$
2-jet	Jet 1	2.8 – 3.4	307.5	13.2	1 259 717	3.09	$^{+9.1}_{-9.1}$	1.2	11.8	0.7	11.9	$^{+15.0}_{-15.0}$
2-jet	Jet 1	3.4 – 4.0	95.5	4.5	1 259 717	2.83	$^{+18.2}_{-18.3}$	5.2	16.3	21.2	27.2	$^{+32.7}_{-32.8}$
2-jet	Jet 2	1.0 – 1.6	41.9	2.6	1 259 717	2.12	$^{+45.6}_{-43.1}$	33.6	36.4	24.2	55.1	$^{+71.6}_{-70.0}$
2-jet	Jet 2	1.6 – 2.2	219.4	10.4	1 259 717	2.78	$^{+14.2}_{-14.0}$	7.3	25.5	9.4	28.2	$^{+31.5}_{-31.5}$
2-jet	Jet 2	2.2 – 2.8	392.4	15.5	1 259 717	3.34	$^{+8.9}_{-8.8}$	4.4	6.9	8.0	11.4	$^{+14.5}_{-14.4}$
2-jet	Jet 2	2.8 – 3.4	244.9	12.6	1 259 717	2.57	$^{+10.7}_{-10.5}$	1.3	6.7	8.5	10.9	$^{+15.2}_{-15.1}$
2-jet	Jet 2	3.4 – 4.0	94.4	4.2	1 259 717	3	$^{+18.4}_{-18.6}$	4.1	31.0	9.4	32.6	$^{+37.4}_{-37.6}$
3-jet	Jet 1	1.0 – 1.6	31.1	3.2	889 570	1.8	$^{+52.9}_{-49.7}$	22.4	95.7	20.3	100.4	$^{+113.5}_{-112.0}$
3-jet	Jet 1	1.6 – 2.2	131.6	9.4	889 570	2.63	$^{+18.4}_{-18.1}$	0.4	12.3	1.6	12.4	$^{+22.2}_{-22.0}$
3-jet	Jet 1	2.2 – 2.8	312.2	18.5	889 570	3.16	$^{+9.7}_{-9.6}$	3.9	3.1	3.8	6.2	$^{+11.6}_{-11.4}$
3-jet	Jet 1	2.8 – 3.4	210.4	12.7	889 570	3.1	$^{+11.6}_{-11.5}$	4.9	5.8	8.4	11.3	$^{+16.2}_{-16.1}$
3-jet	Jet 1	3.4 – 4.0	49.1	5.4	889 570	1.71	$^{+28.3}_{-27.7}$	10.7	35.2	6.8	37.4	$^{+46.9}_{-46.5}$
3-jet	Jet 2	1.0 – 1.6	23.1	2.8	889 570	1.52	$^{+59.1}_{-54.5}$	26.2	87.0	11.3	91.6	$^{+109.0}_{-106.6}$
3-jet	Jet 2	1.6 – 2.2	188.5	9.9	889 570	3.56	$^{+14.1}_{-13.9}$	3.0	11.4	8.5	14.6	$^{+20.3}_{-20.1}$
3-jet	Jet 2	2.2 – 2.8	347.1	17.4	889 570	3.74	$^{+9.5}_{-9.4}$	0.8	18.9	8.7	20.8	$^{+22.9}_{-22.8}$
3-jet	Jet 2	2.8 – 3.4	183.4	12.7	889 570	2.7	$^{+13.0}_{-12.9}$	1.9	6.1	7.0	9.5	$^{+16.1}_{-16.0}$
3-jet	Jet 2	3.4 – 4.0	33.0	3.9	889 570	1.58	$^{+38.2}_{-38.4}$	9.8	58.3	27.4	65.2	$^{+75.6}_{-75.7}$
3-jet	Jet 3	1.0 – 1.6	0.0	3.9	889 570	< 0.266	–	–	–	–	–	–
3-jet	Jet 3	1.6 – 2.2	125.0	13.2	889 570	1.77	$^{+15.8}_{-15.5}$	5.4	20.4	4.6	21.6	$^{+26.8}_{-26.6}$
3-jet	Jet 3	2.2 – 2.8	347.6	19.6	889 570	3.33	$^{+8.8}_{-8.6}$	1.6	11.9	5.6	13.3	$^{+15.9}_{-15.8}$
3-jet	Jet 3	2.8 – 3.4	289.7	14.3	889 570	3.79	$^{+9.7}_{-9.6}$	3.1	13.1	0.5	13.4	$^{+16.6}_{-16.5}$
3-jet	Jet 3	3.4 – 4.0	67.2	5.8	889 570	2.19	$^{+22.3}_{-21.9}$	10.3	36.2	4.8	38.0	$^{+44.0}_{-43.9}$